

SI Appendix, Figures S1 to S15, Tables S1, and Materials and Methods.

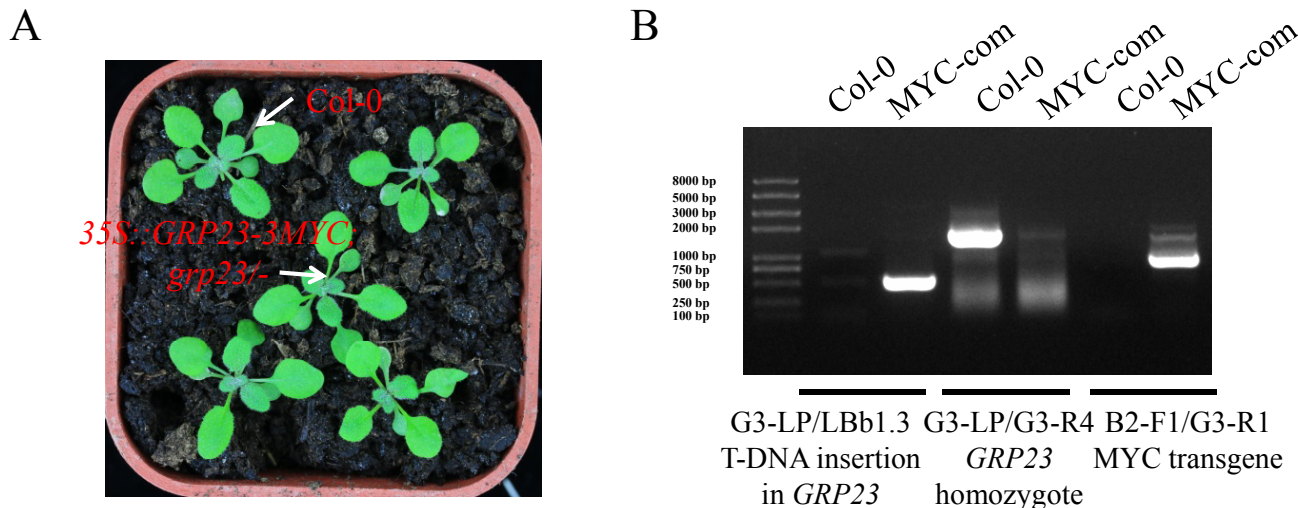


Fig. S1. Complementation of *grp23* mutants with 35S::*GRP23-3MYC*.

(A) Phenotypes of the wild type and the *grp23* mutant complemented by 35S::*GRP23-3MYC*. Images of 3-week-old seedlings were taken. (B) Genotype of the complemented *grp23* mutant. Primer pair G3-LP/LBb1.3 is used to identify the T-DNA insertion in *grp23*; G3-LP/G3-R4 is used to identify the *grp23* homozygote; B2-F1/G3-R1 is used to identify the *GRP23-3MYC* transgene.

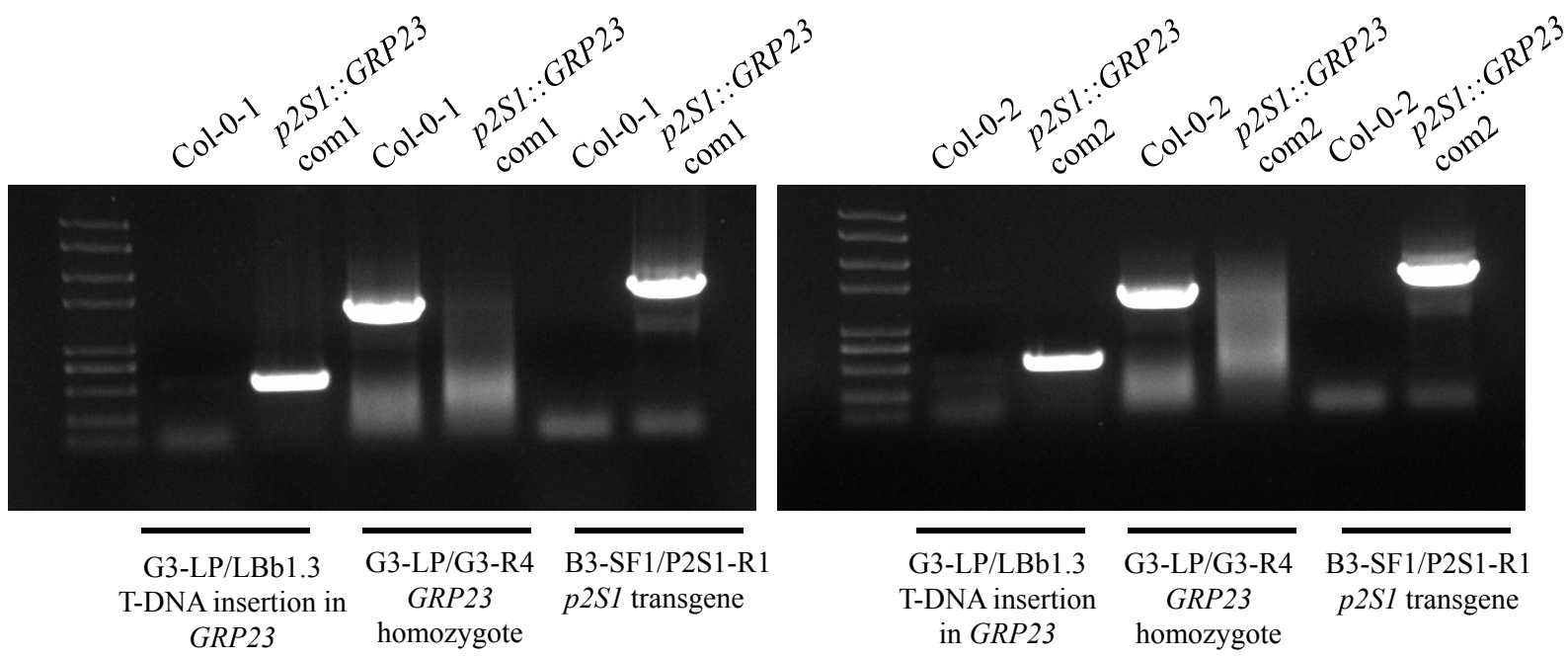
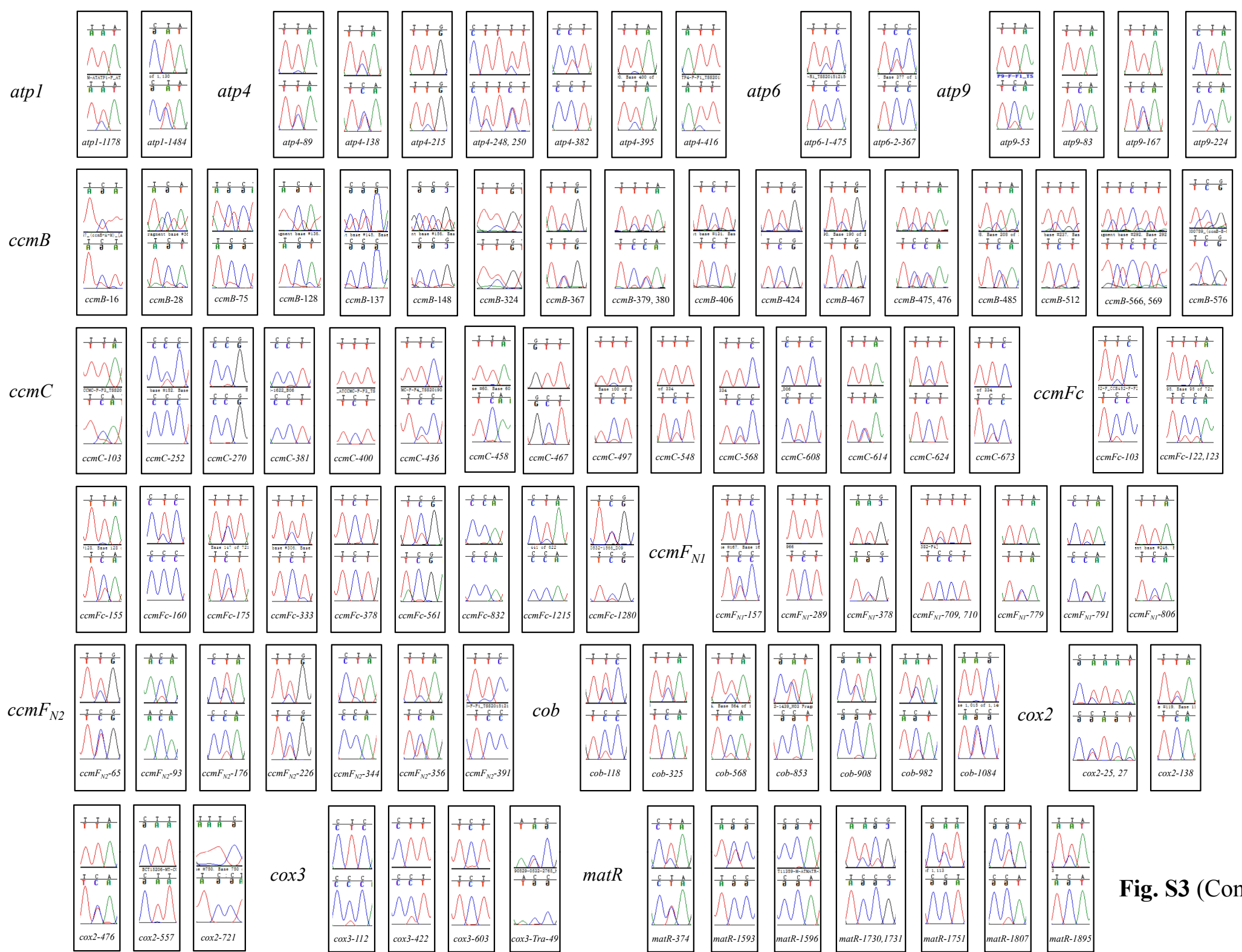
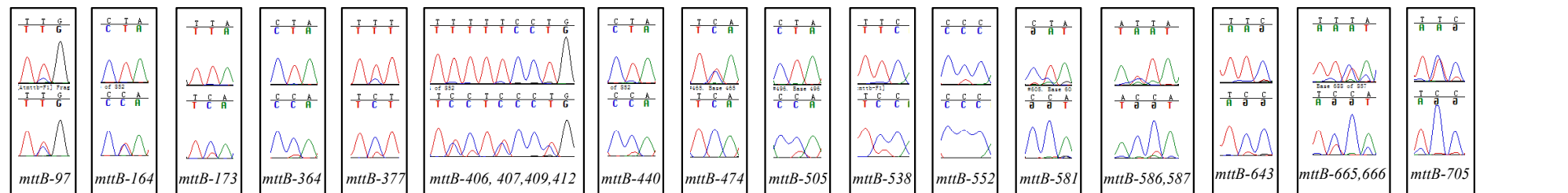
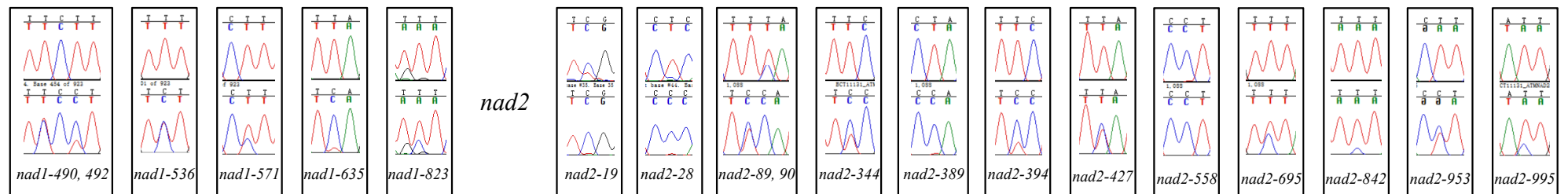
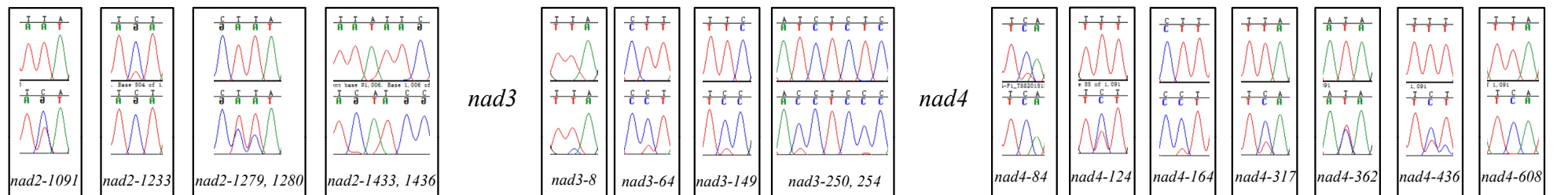
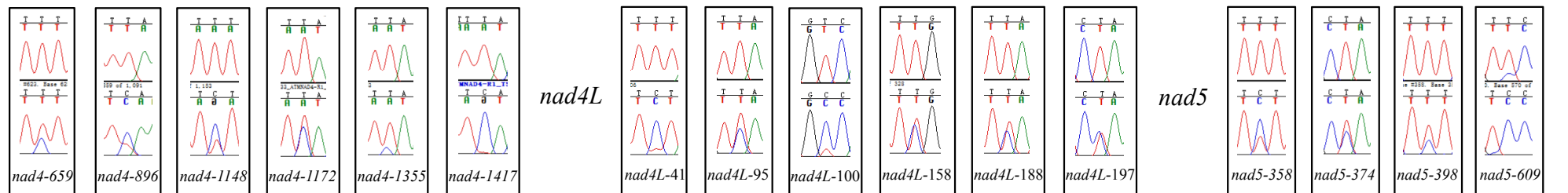
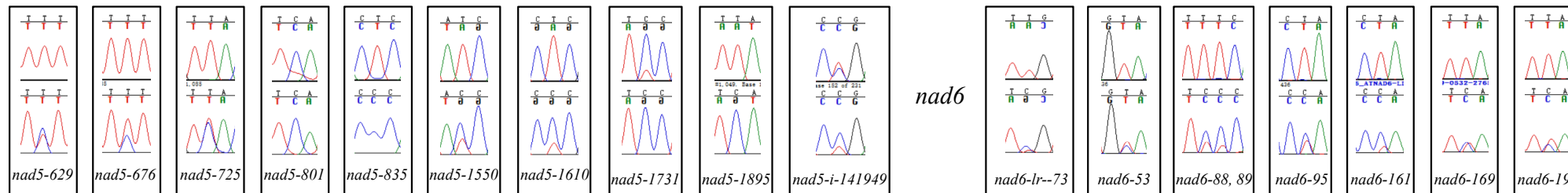


Fig. S2. Genotype of the *grp23* mutants complemented by *p2S1::GRP23*.

Primer pair G3-LP/LBb1.3 is used to identify the T-DNA insertion in *grp23*; G3-LP/G3-R4 is used to identify the *grp23* homozygote; B3-SF1/P2S1-R1 is used to identify the *p2S1::GRP23* transgene.



mttB*nad1**nad2**nad3**nad4**nad5***Fig. S3 (Continued)**

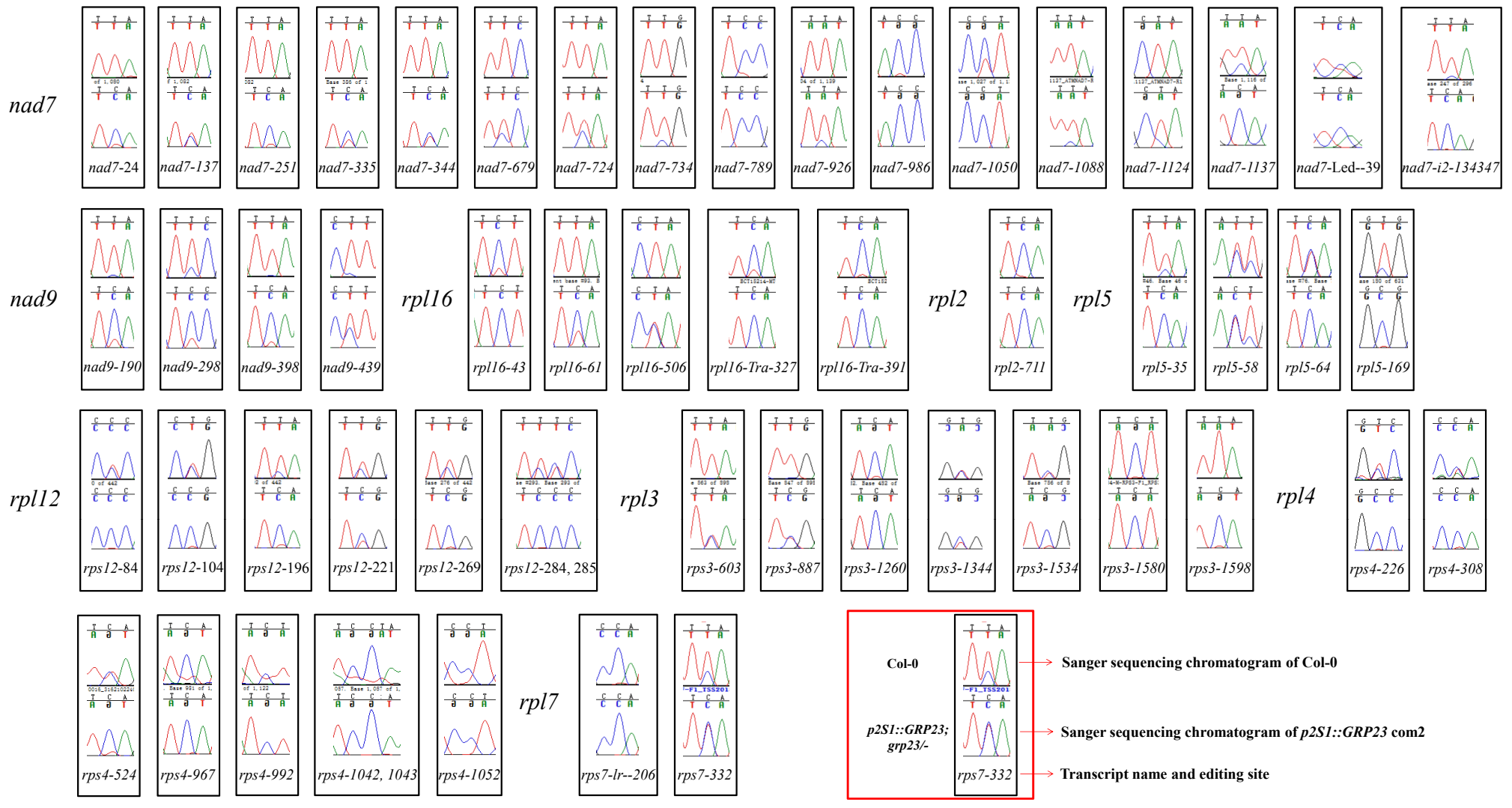


Fig. S3. Editing analysis of *p2S1::GRP23* com2 by Sanger sequencing of targeted RT-PCR products.

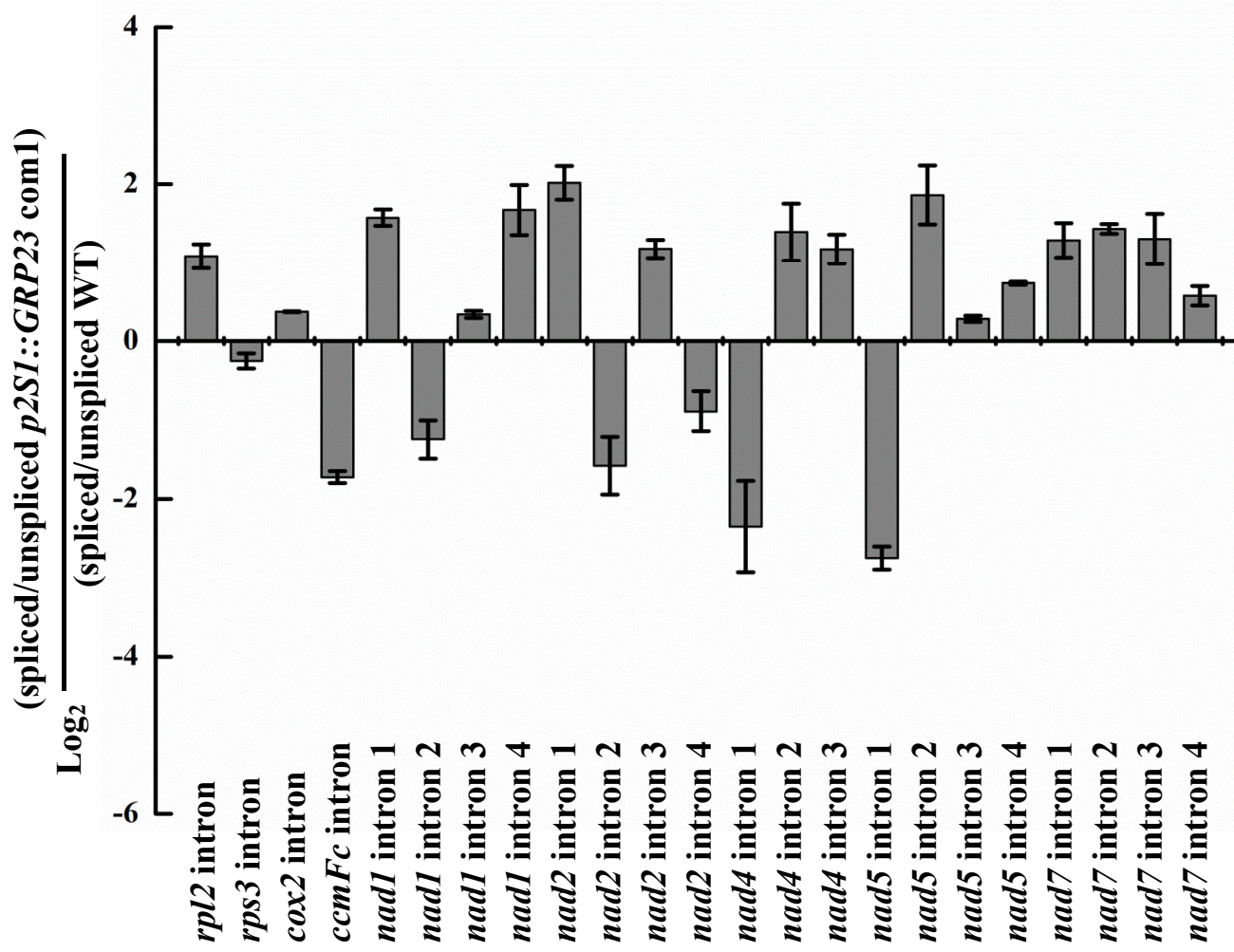


Fig. S4. Splicing efficiency of mitochondrial introns in the *p2S1::GRP23 com1* mutants.

The splicing efficiency of 23 introns of mitochondrial genes in the *p2S1::GRP23 com1* was detected by quantitative RT-PCR. Values are the mean \pm SE of three biological repeats.

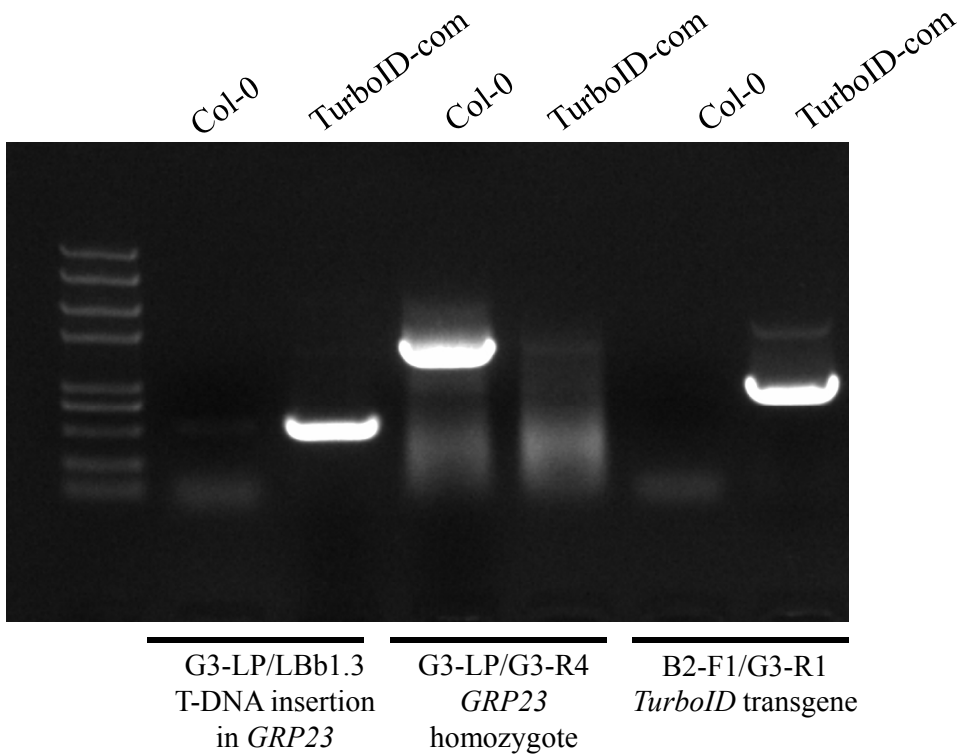
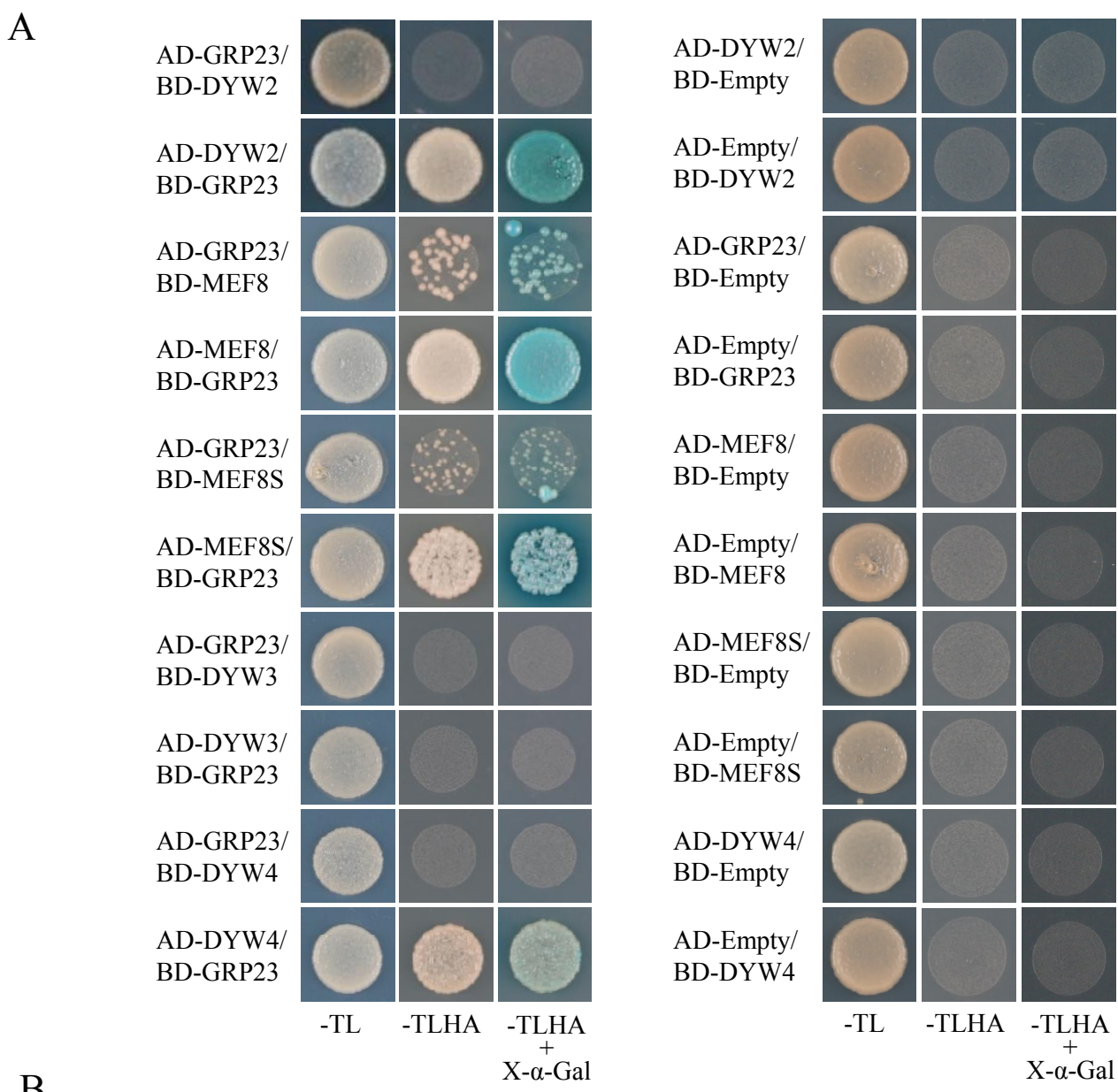


Fig. S5. Genotype of the *grp23* mutant complemented by *p35S::GRP23-TurboID*.

Primer pair G3-LP/LBb1.3 is used to identify the T-DNA insertion in *grp23*; G3-LP/G3-R4 is used to identify the *grp23* homozygote; B2-F1/G3-R1 is used to identify the *GRP23-TurboID* transgene.



B

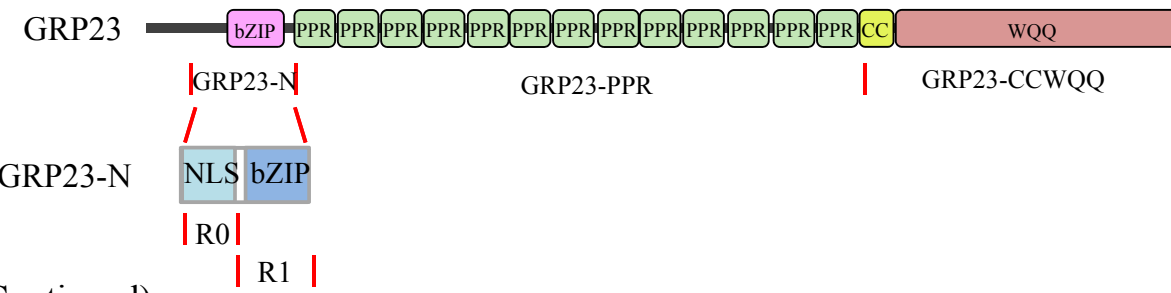
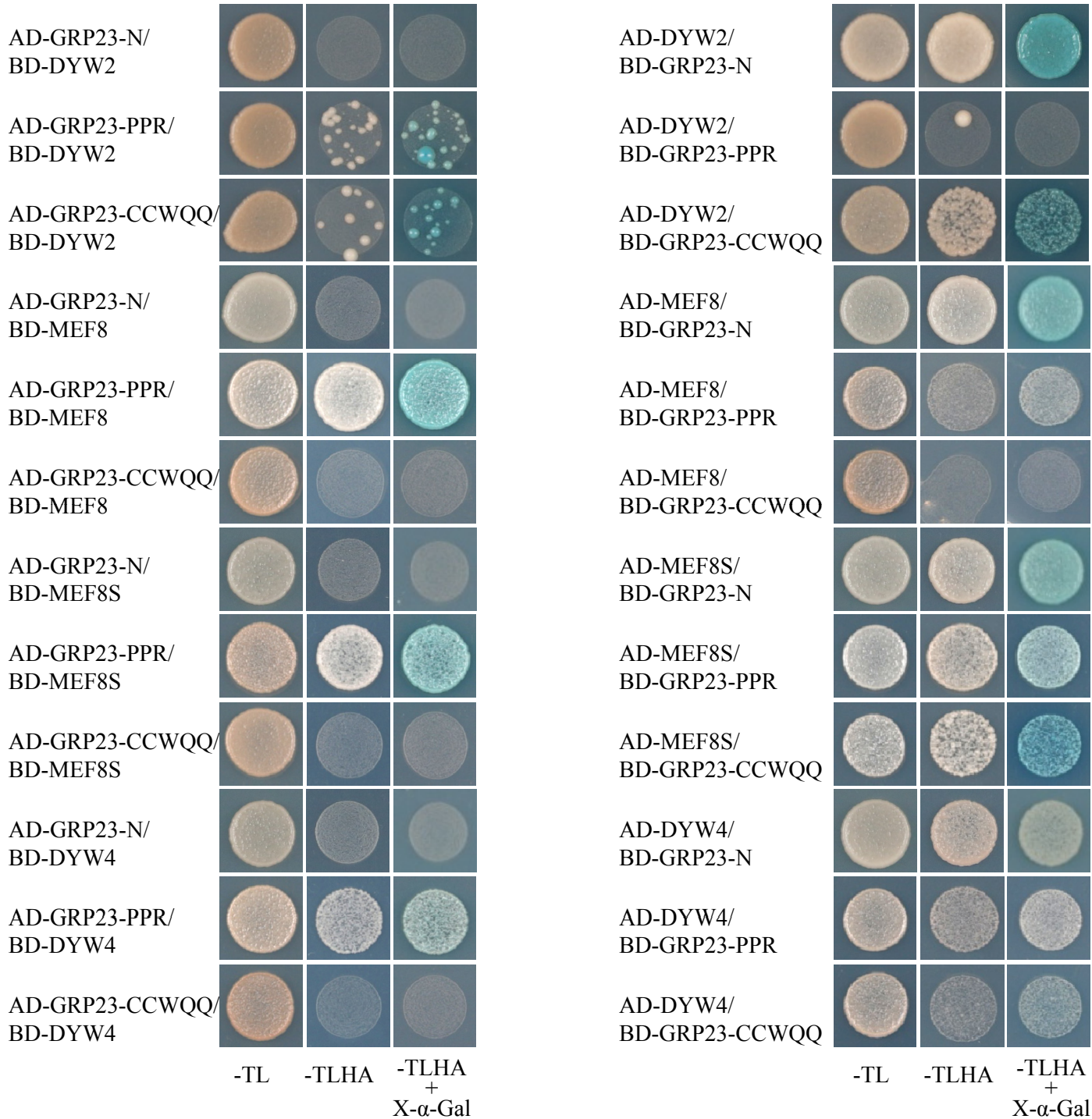
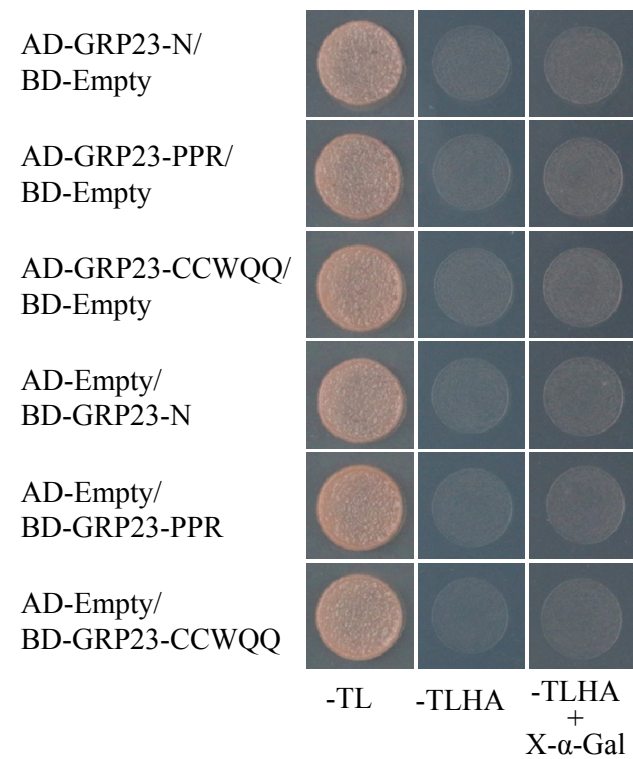


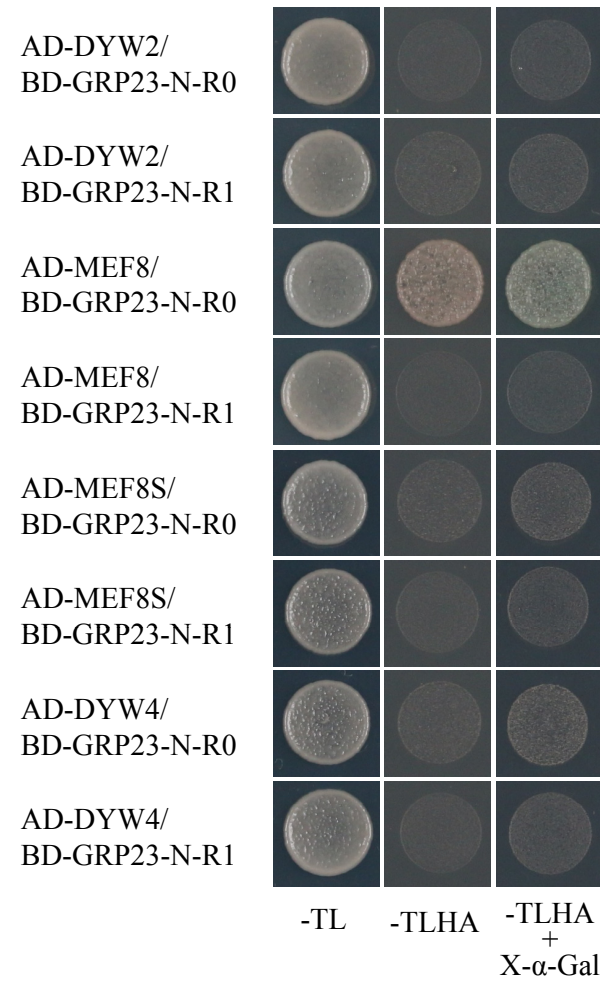
Fig. S6. (Continued)

C

**Fig. S6.** (Continued)



-TL -TLHA -TLHA
+
X- α -Gal



-TL -TLHA -TLHA
+
X- α -Gal

Fig. S6. (Continued)

D

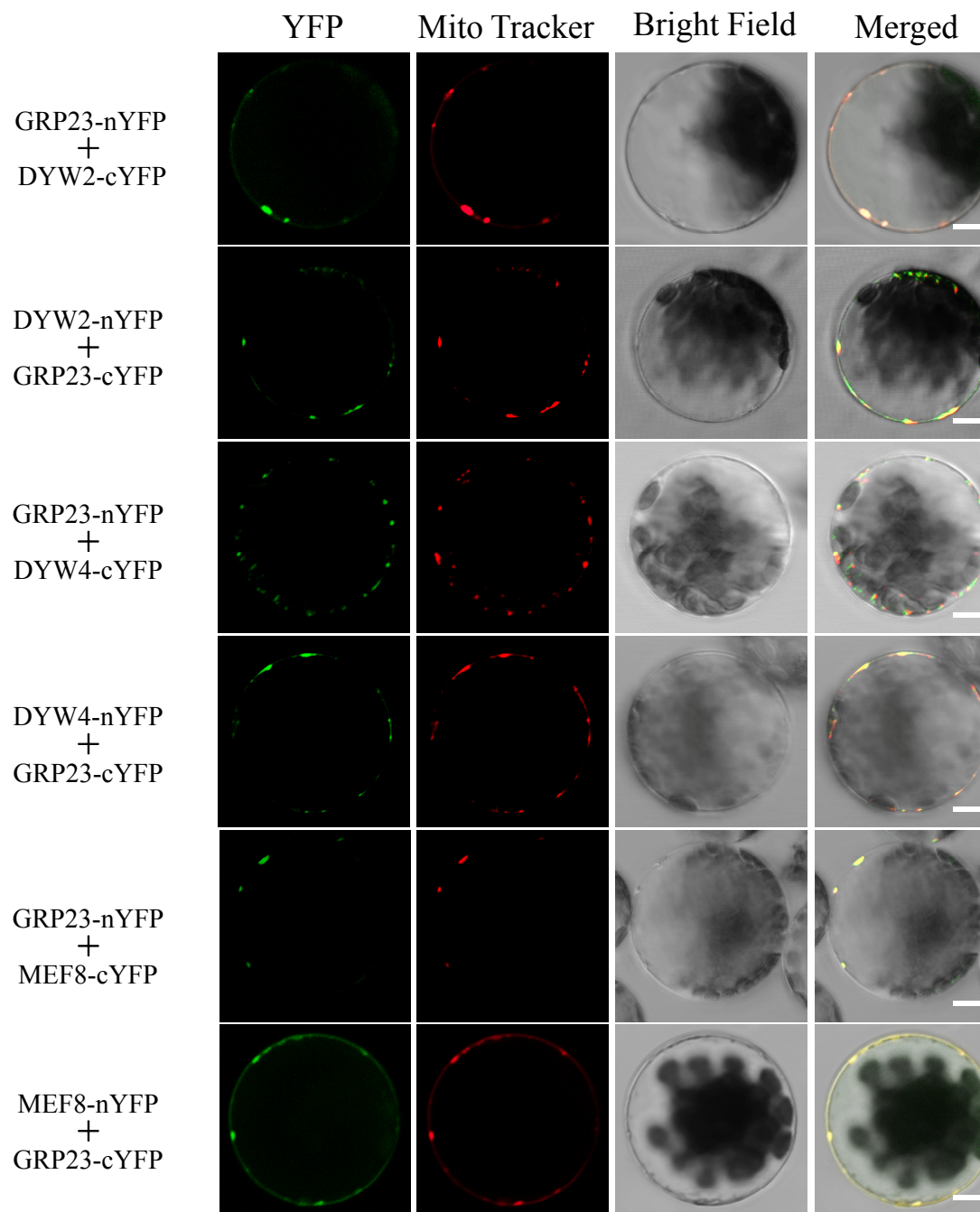


Fig. S6. (Continued)

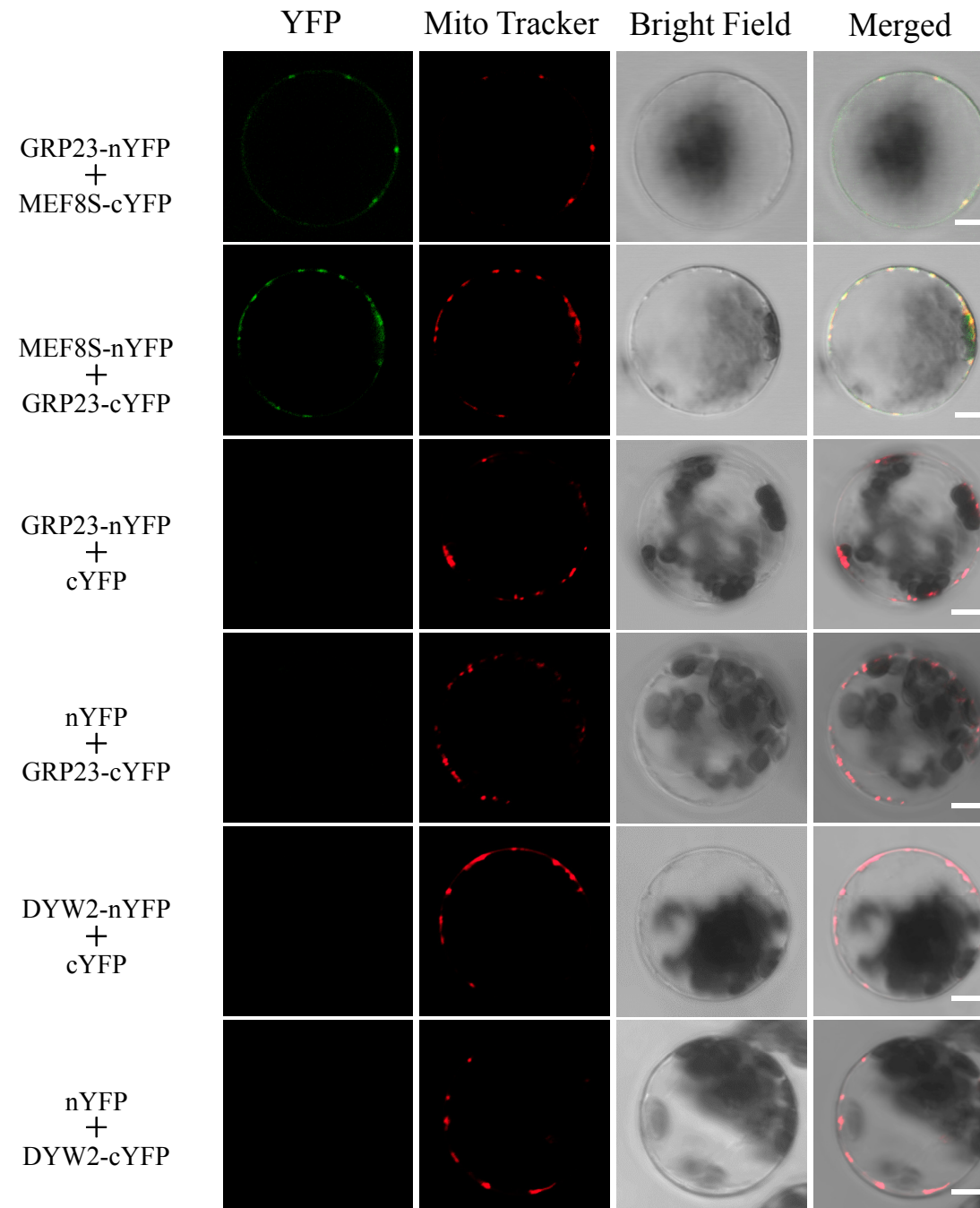


Fig. S6. (Continued)

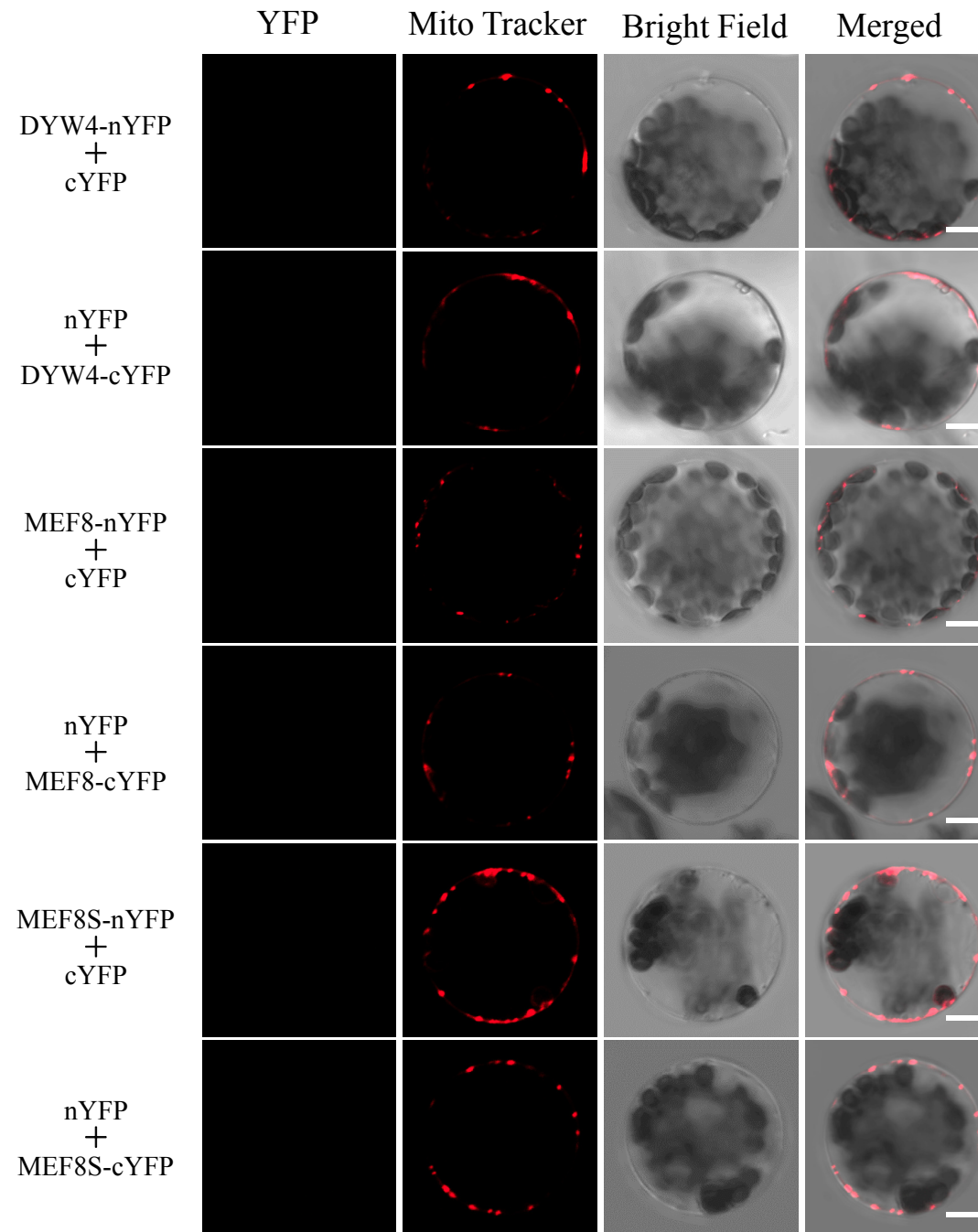


Fig. S6. (Continued)

Fig. S6. GRP23 interacts with atypical PPR-DYWs in yeast and *Arabidopsis* protoplasts.

(A) GRP23 interacts with DYW2, MEF8, MEF8S, and DYW4 in yeast. -TL, -TLHA and -TLHA+X- α -Gal indicate SD/-Trp-Leu, SD/-Trp-Leu-His-Ade, and SD/-Trp-Leu-His-Ade containing X- α -Gal dropout plates, respectively. AD-Empty, pGADT7 empty vector. BD-Empty, pGBKT7 empty vector. Images were taken after 3 days of incubation at 30 °C. (B) Diagram of the truncations of GRP23 used in Y2H. (C) The N-terminal region and PPR motif of GRP23 interact with DYW2, MEF8, MEF8S, and DYW4. (D) BiFC analysis shows the interactions between GRP23 and DYW2, MEF8, MEF8S, and DYW4 in *Arabidopsis* mitochondria. Scale bars = 5 μ m.

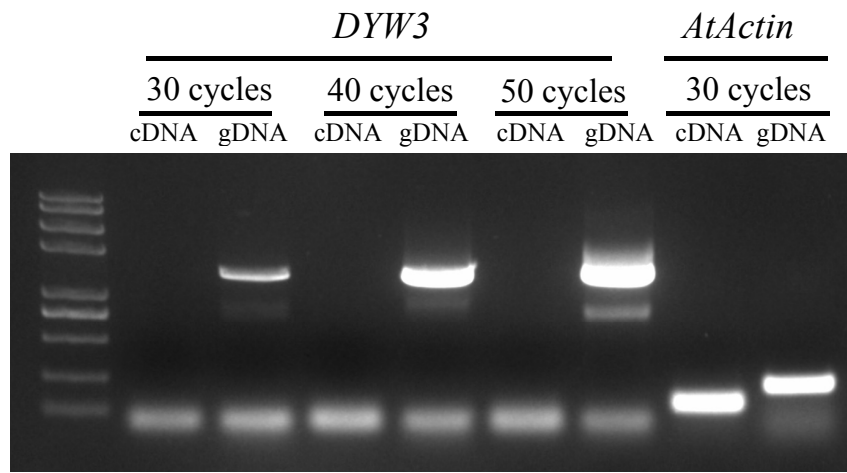
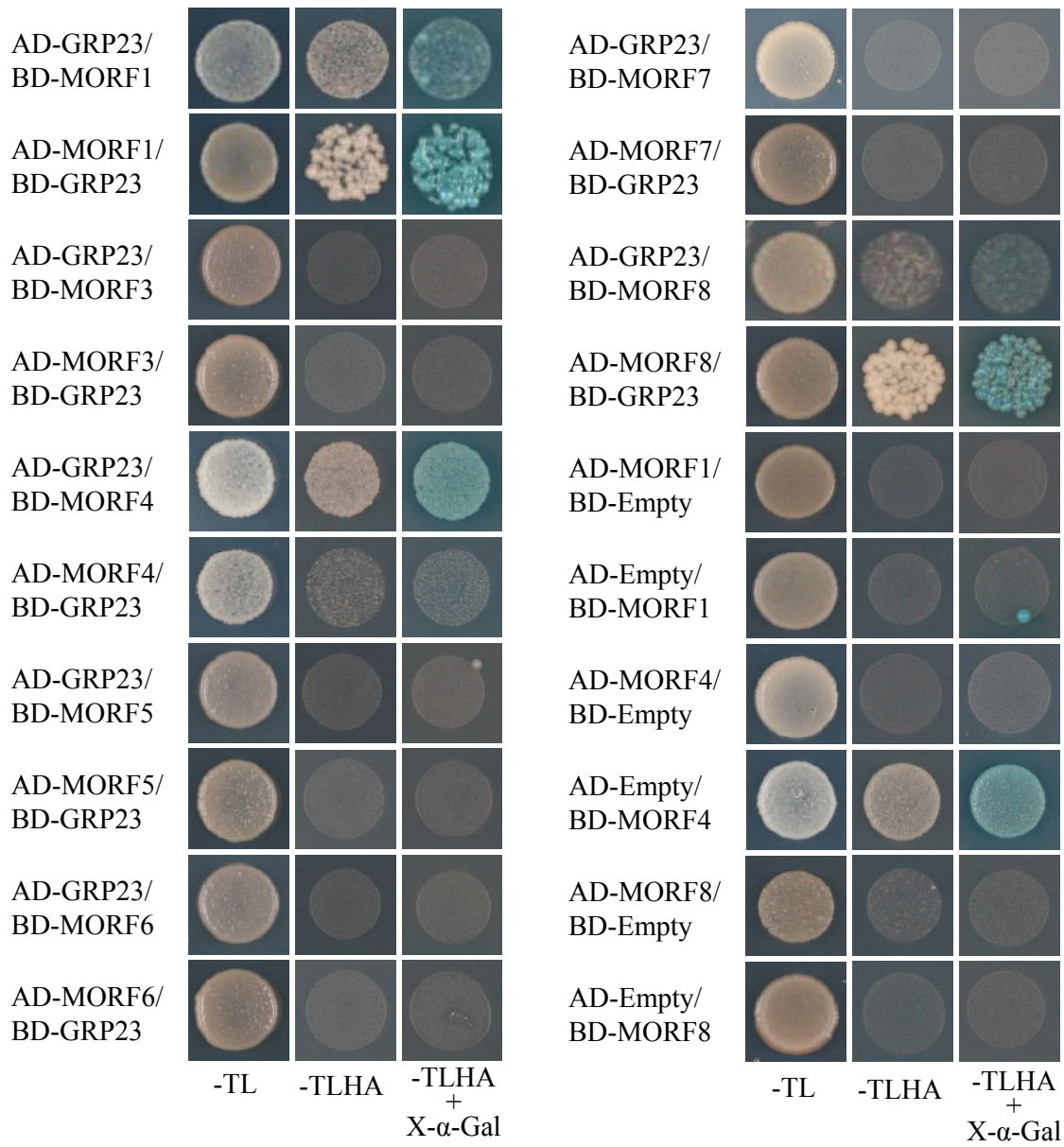


Fig. S7. *DYW3* is not expressed in *Arabidopsis*.

The expression of *DYW3* was detected by RT-PCR. Reverse transcription reactions were performed using 1 µg of total RNA from total seedling with random hexamers by SuperScript II Reverse Transcriptase (Invitrogen). PCR was performed with 0.1 µg *Arabidopsis* genomic DNA as a positive control.

A**Fig. S8** (Continued)

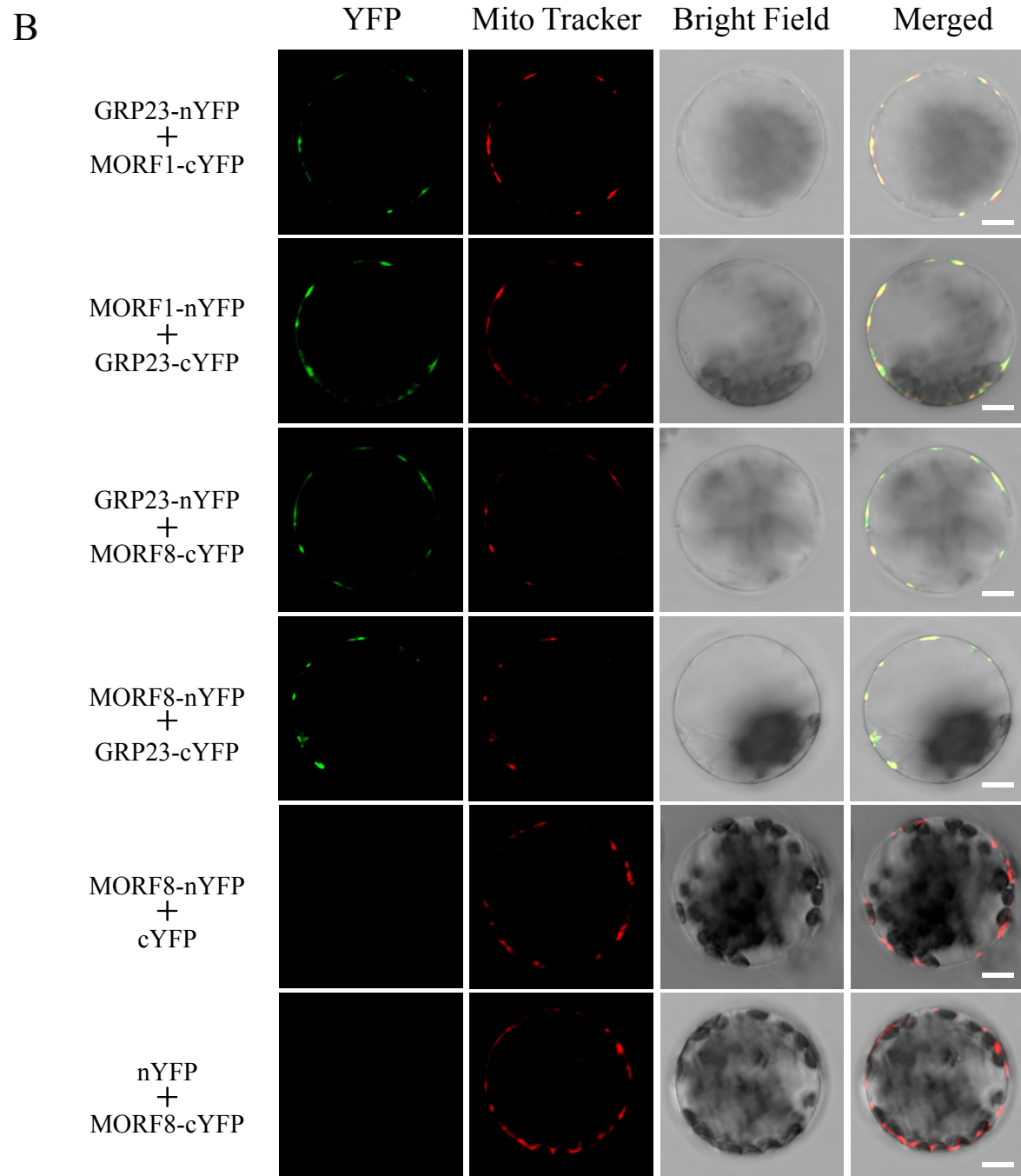


Fig. S8 (Continued)

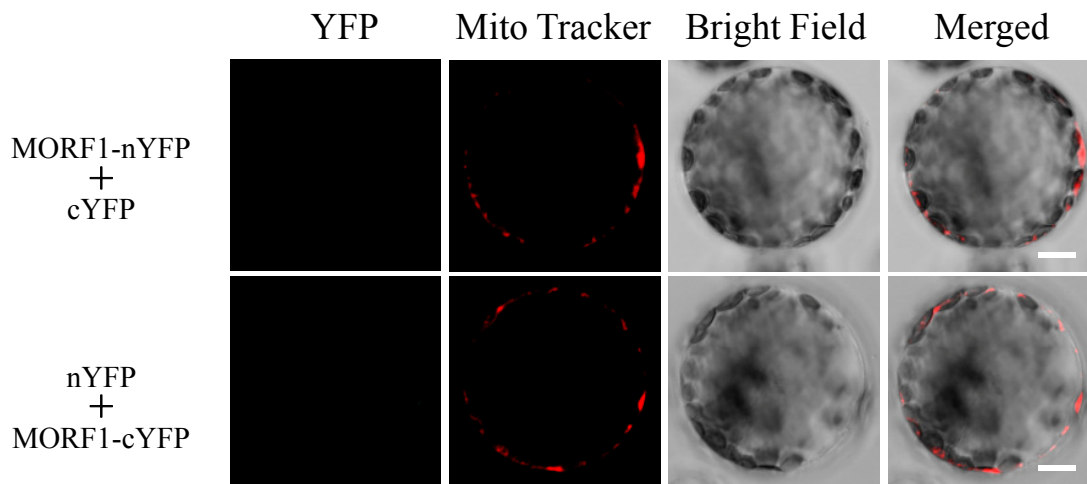


Fig. S8. GRP23 interacts with MORF1 and MORF8 in yeast and Arabidopsis protoplasts.

(A) Detection of the interactions between GRP23 and MORFs in yeast. MORF4 fused to BD shows strong auto-activation for HIS and ADE reporters. Images were taken after 3 days of incubation at 30 °C. -TL, -TLHA, and -TLHA+X- α -Gal indicate SD/-Trp-Leu, SD/-Trp-Leu-His-Ade, and SD/-Trp-Leu-His-Ade containing X- α -Gal dropout plates, respectively. B. BiFC analysis shows the interactions between GRP23 and MORF1 and MORF8 in Arabidopsis mitochondria. Scale bars = 5 μ m.

A

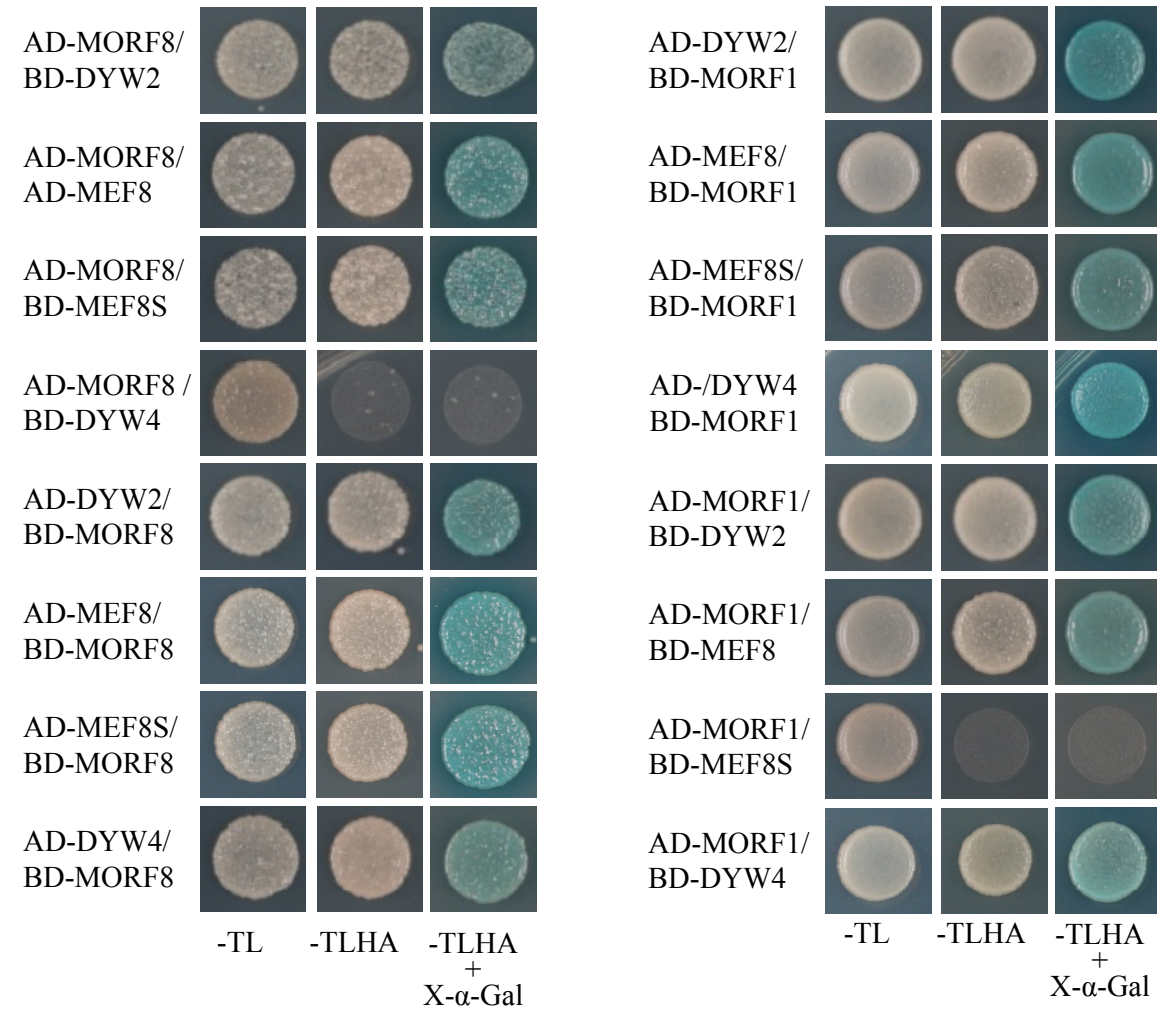


Fig. S9 (Continued)

B

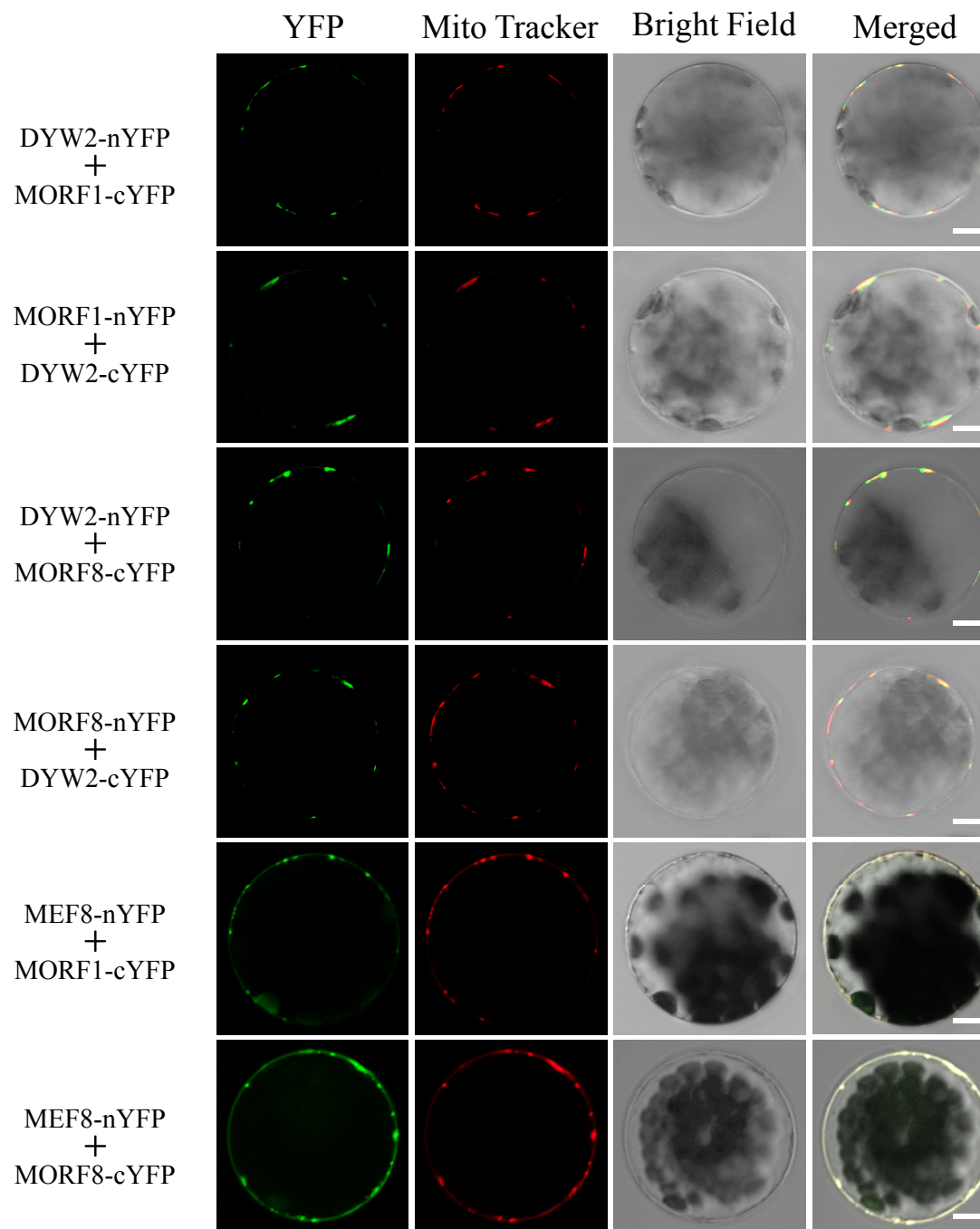


Fig. S9 (Continued)

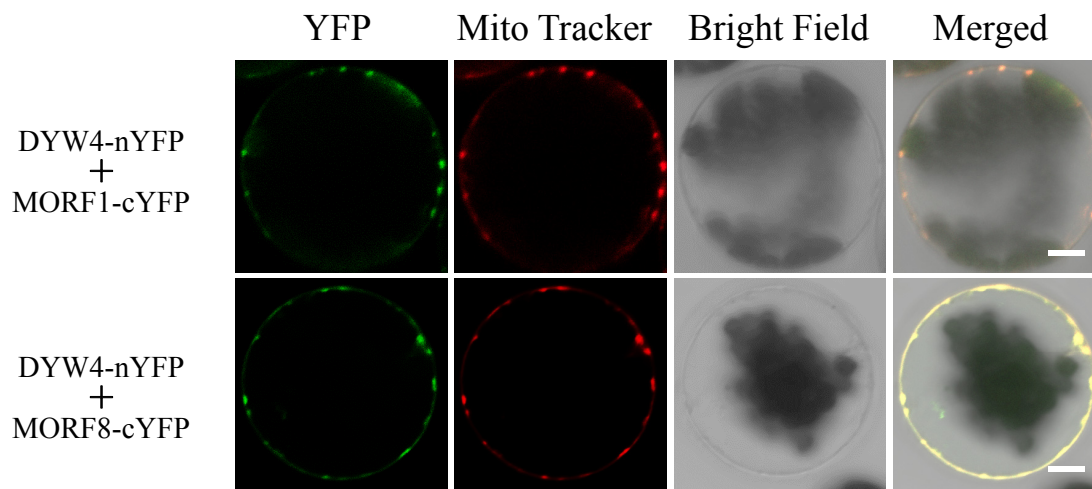


Fig. S9. MORF1 and MORF8 interact with atypical PPR-DYW proteins DYW2, MEF8, MEF8S, and DYW4.

(A) MORF1 and MORF8 interact with PPR-DYW proteins DYW2, MEF8, MEF8S, and DYW4 in yeast. -TL, -TLHA, and -TLHA+X- α -Gal indicate SD/-Trp-Leu, SD/-Trp-Leu-His-Ade, and SD/-Trp-Leu-His-Ade containing X- α -Gal dropout plates, respectively. (B) BiFC analysis shows the interactions between MORF1 and MORF8 with atypical PPR-DYWs DYW2, MEF8, and DYW4 in *Arabidopsis* mitochondria. Scale bars = 5 μ m.

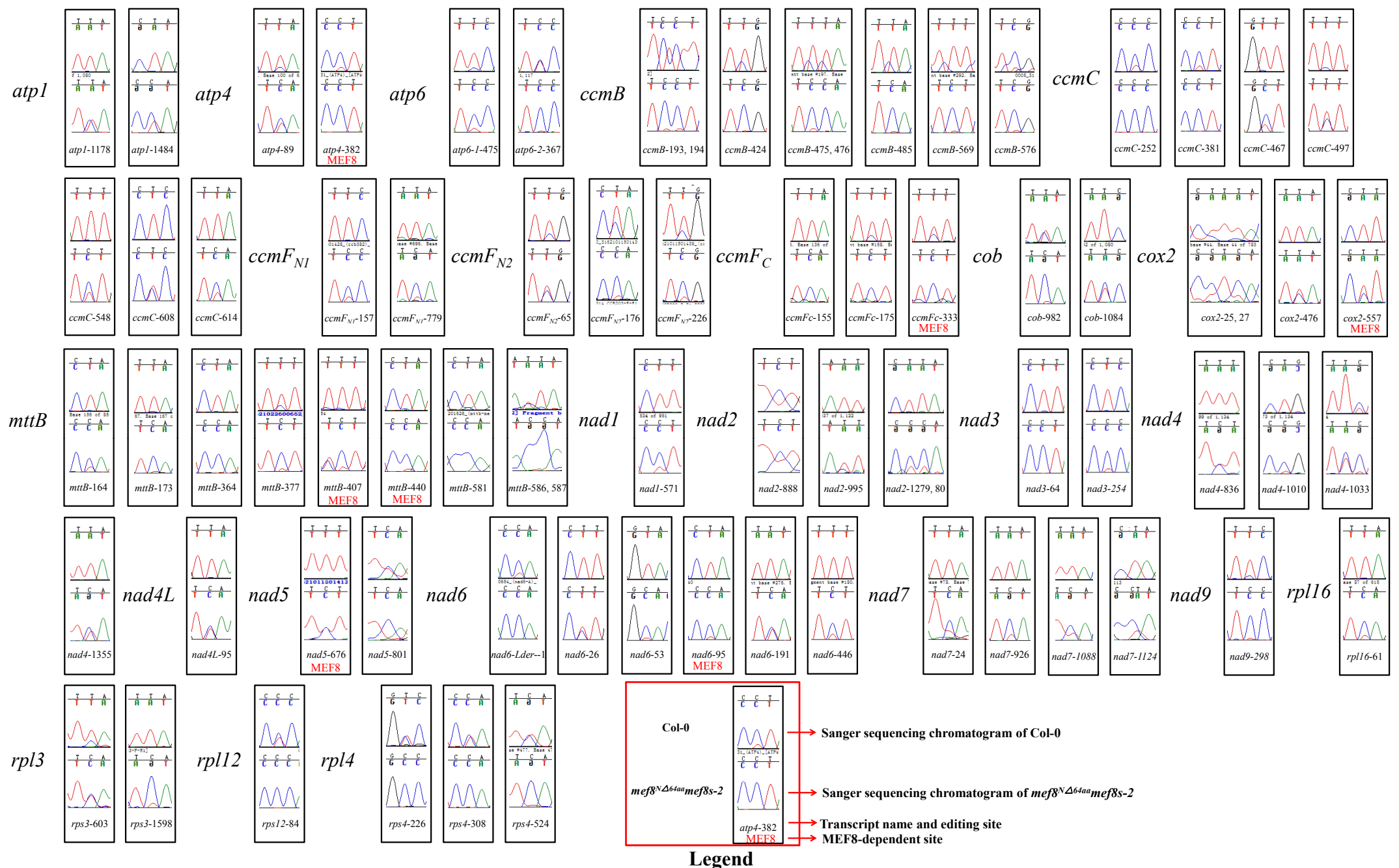


Fig. S10. Editing analysis of *mef8^{NΔ64aa}mef8s-2* by Sanger sequencing of targeted RT-PCR products.

A

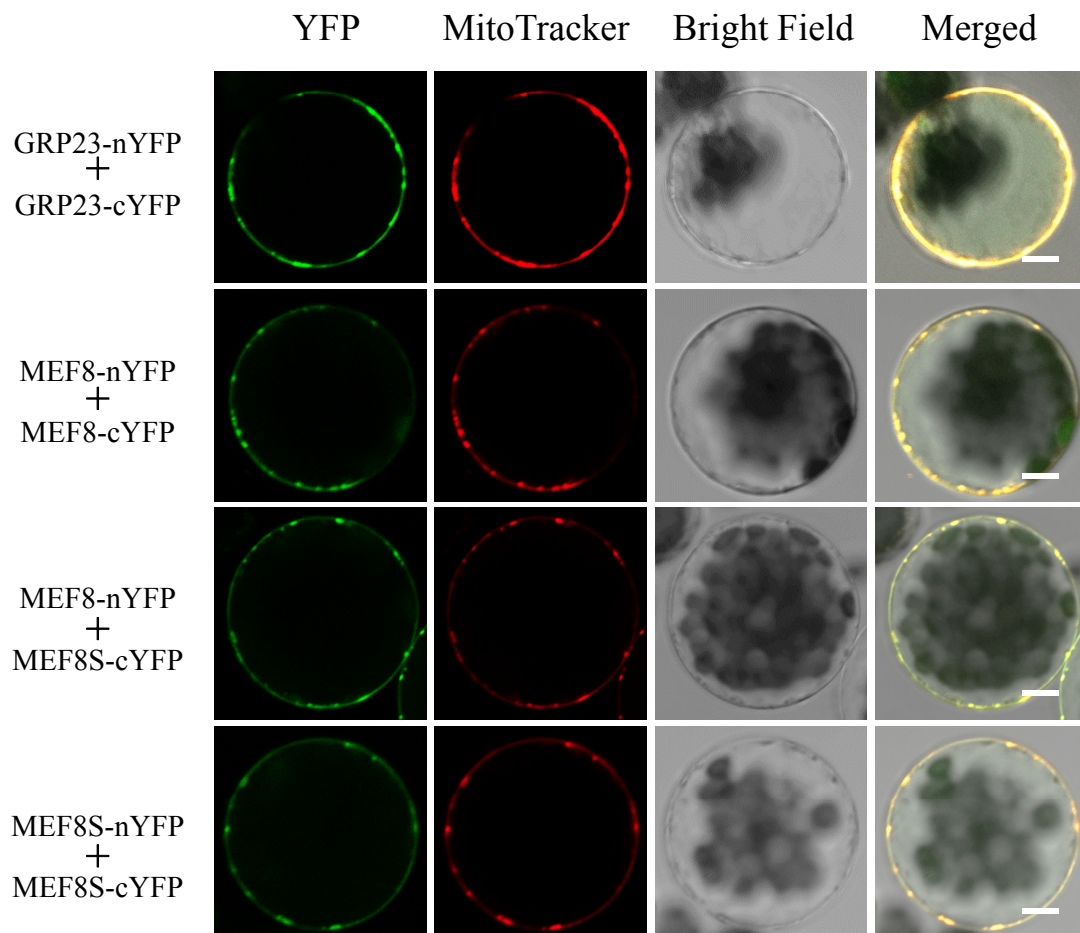


Fig. S11 (Continued)

B

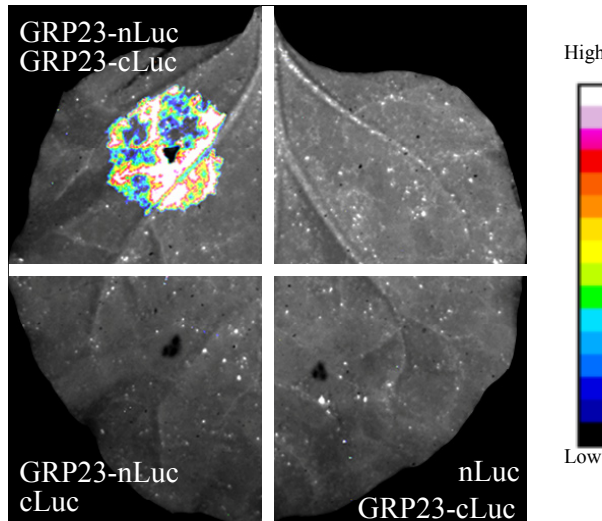


Fig. S11. GRP23 and MEF8/MEF8S form dimers.

(A) Detection of the dimerization of GRP23 and MEF8/MEF8S by BiFC assay. Arabidopsis protoplasts were transfected with the combination of GRP23-nYFP/GRP23-cYFP, MEF8-nYFP/MEF8-cYFP, MEF8-nYFP/MEF8S-cYFP, and MEF8S-nYFP/MEF8S-cYFP constructs and observed by confocal microscopy 18-22 hours after transfection. Scale bars = 5 μ m. (B) Detection of GRP23 homodimer by LUC assay. Tobacco leaves were infiltrated with Agrobacterium containing GRP23-NLuc and GRP23-CLuc constructs. The signals were captured by a Lumazone Pylon 2048B system 2 days after infiltration.

		NLS	
GRP23	78	IPYPPPIPHRTMAFSSAEEEAAERRRRKRRRLRIEPPPLHALRRD---PSAPPKRDPNAPR +P P + R M+F++ EAAAERRRRKRRRLR+EPP+++ R P P ++PN P+	133
NUWA	24	LPQPFLAVRYMSFATOEEAAAERRRRKRRRLMEPPVNSFNRSQQQQSQIPRPIQNPNIKP bZIP	83
GRP23	134	bZIP LPDSTSALVGQRNLHNRVQSLIRASDLDAASKLARQSFSNTRPTVFTCNAAIAAMYRA LP+S SALVG+RL+LHN + LIR +DL+ A+ R SV+SN RPT+FT N ++AA R	193
NUWA	84	LPESVSALVGKRLDLHNHILKLIRENDLEEAALYTRHSVYSNCRPTIFTVNTVIAAQLRQ PPR	143
GRP23	194	KRYSESISLFQYFFKQSNIVPNVVSYNQIINAHCDEGNVDEALEVYRHILANAPFAPSSV +Y + L F Q+ I PN+++YN I A+ D + ALE Y+ + NAP PS	253
NUWA	144	AKYGALLQL-HGFINQAGIAPNIITYNLIFOAYLDVRKPEIALEHYKLFIDNAPLNPSIA PPR	202
GRP23	254	PPR TYRHLTKGLVQAGRIGDAASLLREMLSKGQAADSTVYNNLIRGYLDLGDFDKAVEEFFDEL T+R L KGLV + A + +M KG D VY+ L+ G + D D ++ + EL	313
NUWA	203	TFRILVKGLVSNDNLEKAMEIKEDMAVKGFVVDPVVSYLMMGCVKNSADGVLKLYQEL PPR	262
GRP23	314	KSKC--TVYDGIVNATFMEYWFEKGNDKEAMESYRSLL--DKKFRMHPPPTGNVLLEVFLK K K V DG+V M+ +F K +KEAME Y + + K RM N +LE +	369
NUWA	263	KEKLGGFVDDGVVYQQLMKGYFMKEMEKEAMECYEEAVGENSKVRMSAMAYNYVLEALSE PPR	322
GRP23	370	PPR FGKKDEAWALFNEMLDNHAPPNILSVNSDTVGIMVNNECFKMGEFSEAINTFKKVGSKVTS GK DEA LF+ + H PP L+VN T +MVN G+F EA+ F+++G S	429
NUWA	323	NGKFDEALKLFDALKKEHNPPRHLAVNLGTNFNVMVNGYCAGGKFEAEAMEVFRQMGDFKCS PPR	382
GRP23	430	KPFVMDYLGYCNIVTRFCEQGMLTEAERFFAEGVSRSLPADAPSHRAMIDAYLKAERIDD D L + N++ + C+ +L EAE+ + E +++ D ++ ++D K +ID+ PPR	489
NUWA	383	P----DTLSFNNLMNQLCDNELLAEAEKLYGEMEEKNVPDETYGLLMDTCFKEGKIDE PPR	438
GRP23	490	PPR AVKMLDRMVDVNLRVVADEFGARVFGELIKNGKLTESAEVLTKMGEREPKPDPSIYDVVVR MV+ NLR R+ +LIK GKL ++ M + K D Y ++R	549
NUWA	439	GAAYYKTMVESNLRPNLAVYNRLQDQLIKAGKLDDAKSFFDMMVSK-LKMDDEAYKFIMR coiled-coil PPR	497
GRP23	550	GLCDGDALDQAKDIVGEMIRHN--VGVTTVLREFIIEVFEKAGRREEIEKILNSVARPVRN L + LD+ IV EM+ + V V+ L+EF+ E K GR ++EK++ R	608
NUWA	498	ALSEAGRLDEMLKIVDEMLDDDTVRVSEELQEfvKEELRKGGREGDILEKLMEEKERLKAE coiled-coil	557
GRP23	609	A-----GQSGNTPPRVPAVFGTPAAPQQPRDRAP--WTSQGVVHSNSGWAN A QS N +P P A ++ ++ A W ++ +	653
NUWA	558	AKAKELADAEEKKQAQSINTIAALIP-----PKAVEEKKETAKLLWENEAGGVEEADVVE	611
GRP23	654	GTAGQTAGGAYKANNQNP 672 G AGG+ NGQ+P	
NUWA	612	MAKGVEAGGS----NGQDP 626	

Fig. S12. Alignment of partial GRP23 and NUWA protein sequences.

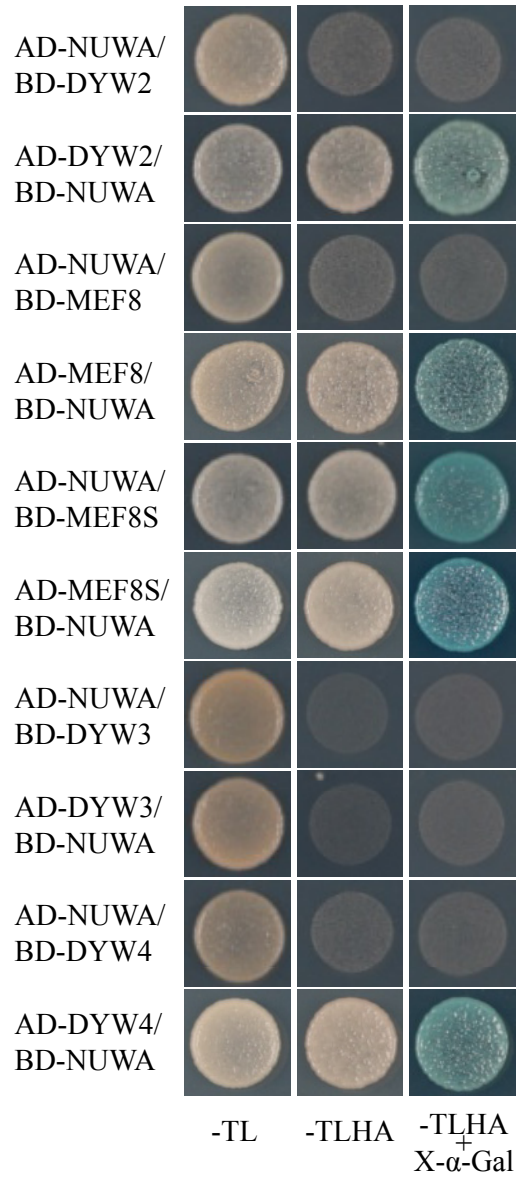


Fig. S13. NUWA interacts with atypical PPR-DYWs in yeast.

-TL, -TLHA and -TLHA+X- α -Gal indicate SD/-Trp-Leu, SD/-Trp-Leu-His-Ade, and SD/-Trp-Leu-His-Ade containing X- α -Gal dropout plates, respectively.

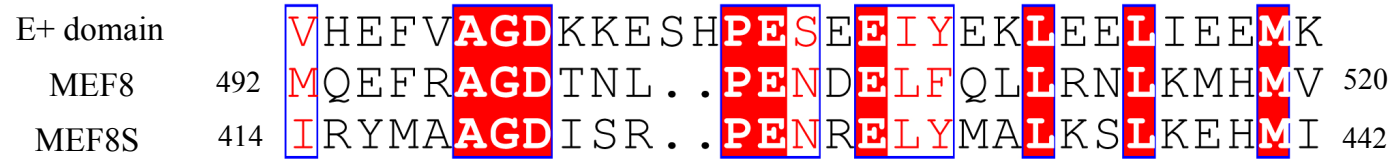


Fig. S14. Comparison of the E+ domains of MEF8 and MEF8S with a consensus sequence of E+ domain.

Red shaded boxes indicate identical residues. Red letters indicate similar residues. The consensus sequence of E+ domain was obtained using the HMMER package based on alignments of 148 E+ domain from Arabidopsis (13).

MEF8	62	RTGSSGEVSESIHTQSQSLGSNQGRNEQSWKQSPSLSNSQVQSQYQGNWYGTNSDYQNGVGSSW	125
MEF8S	62	QSLGGFQQNSYEQSLNPVSGQNPTNRFYQNGYNRNQSYGEHSEIINQRNQNWQSSDGCSSYGT	125
DYW2	62	PQSGSPSQHQRPYPPQSFDSQNQTNTNQRPVQSPNQWSTQHGGQIPQYGGQNPQHGGQRPPYGG	125

Fig. S15. The N-terminal regions of MEF8, MEF8S, and DYW2 are rich in glutamine residue.
The N-terminal regions from 62aa to 125aa of MEF8, MEF8S, and DYW2 are shown. Glutamine residues are labeled in red.

Table S1. Primers used in this study

Primer Name	sequence	Purpose
AtNad9-F-F1	TGAAGAGCAAGAACGGAAAC	STS-Seq
AtNad9-F-R1	TTGATTGTCCCCTGGACTG	STS-Seq
AtRpl16-F-F1	GGTCGATTAAAAGACGCAGC	STS-Seq
AtRpl16-F-R1	AGATTCTCGGCCGCTTAT	STS-Seq
Atccb452-F-F1	GCGCCTCTCTTCTTAG	STS-Seq
Atccb452-F-R1	GTCGAAGAAGTGCCTTGA	STS-Seq
Atrpl5-F-F1	GAGTAGGAGGAGTCAGCTTA	STS-Seq
Atrpl5-F-R1	CGCGAGCAATCTACGTTGT	STS-Seq
AtCob-F-F1	GGTGGGTGAACAAGAGTTGT	STS-Seq
AtCob-F-R1	CTGCTTGTCAATTCTGGTG	STS-Seq
AtNad6-F-F1	GCTGAAGCAAGAACTAGCATG	STS-Seq
AtNad6-F-R1	CTCATCTGCTCACGAATTGG	STS-Seq
AtAtp6-F-F1	TTGACGGAGTGAAGCTGTCT	STS-Seq
AtAtp6-F-R1	TCCATCCCTCGCTTTGTTC	STS-Seq
AtAtp8-F-F1	AAGCTGTCTGGAGGGAATCA	STS-Seq
AtAtp8-F-R1	TCGAGTGCTTACCTACCAG	STS-Seq
AtMatR-F-F1	AAGGGGAGCAAAAAACGAGC	STS-Seq
AtMatR-F-R1	AGTAAACGCCTGTTCGCATC	STS-Seq
AtCox3-F-F1	AGGCCCAAAGATAAAGAGC	STS-Seq
AtCox3-F-R1	TCTTGAAAAGCCGGTTC	STS-Seq
AtCcb382-F-F1	ACCGGATGATGGAAATAACG	STS-Seq
AtCcb382-F-R1	AGTCGAGTCATTAGGGTTC	STS-Seq
AtCcb203-F-F1	TGCTCCCTACGACGGTAAAT	STS-Seq
AtCcb203-F-R1	AGCCAATTGCTGGCTCTGAA	STS-Seq
AtRps12-F-F1	GTGATAGGGCACAAATGGG	STS-Seq
AtRps12-F-R1	TGATTGTTCCACCGACTGAC	STS-Seq
AtNad3-F-F1	TTCGATATGCCGCTTCTCG	STS-Seq
AtNad3-F-R1	CCCATTTGTGCCCTATCAC	STS-Seq
AtAtp9-F-F1	GTAAGAACGACGAGGAATC	STS-Seq
AtAtp9-F-R1	GAGGTGCTGCTTATGAGA	STS-Seq
AtAtp6-2-F-F1	AGTGGTGGTACAGTAGCT	STS-Seq
AtAtp6-2-F-R1	AGACATCCATCCCTCGCTTT	STS-Seq
AtAtp1-F-F1	AAAGCGGTATTCCTCCTTGC	STS-Seq
AtAtp1-F-R1	GCCTCTCCAGTCTTGCTTA	STS-Seq
AtRps7-F-F1	TCGTCATCGAAAGCGGCTT	STS-Seq
AtRps7-F-R1	CTGACTGAATGACGAAGAGC	STS-Seq
AtCox1-F-F1	CTAACCCCTCTGTATAAGG	STS-Seq
AtCox1-F-R1	AGGTTCTTAGTAGCAGTCGG	STS-Seq
Atnad2-F-F1	CGCTGAAGACCGTAACGTAA	STS-Seq
STS-d5-i2-F	CGTACACTTAGTGGCAATCG	STS-Seq
STS-d5-i2-R	TTAACATCACTACGGTCGGG	STS-Seq
STS-d7-i2-F	GGGCTCCTATTGAAAGGCTT	STS-Seq

STS-d7-i2-R	CTCGTAATGGTACCTCGCAA	STS-Seq
AtNad6-Lder-F1	GGGCTTGGAAAGAAGAAAATG	STS-Seq
AtRpl16-Tler-F	GGTTAATGGGGATAAACCGGG	STS-Seq
AtRpl16-Tler-R	GAGAGTTCTTCTCCATAC	STS-Seq
AtRps14-F-F1	GAGACTTACCACTGTGGAG	STS-Seq
AtRps14-F-R1	TTACCTTGCTTGTGGACCAG	STS-Seq
AtRps7-Lder-F1	CTTGTGAGAGAGTTGTGA	STS-Seq
AtRps7-Lder-R1	CGCAATCGTTACTGTCCATC	STS-Seq
orf114-F-F1	CATCCAACGGATGGCTCTAT	STS-Seq
orf114-F-R1	GGAACACCGAGTAGGATCAA	STS-Seq
AtCox2-F-F1	GAAGGAACCTTGCTTTG	STS-Seq
AtCox3-Tler-F1	GGGAGGTATATGAAGGAACG	STS-Seq
AtCox3-Tler-R1	GACCAAGATCTAATTTCGGG	STS-Seq
AtccmB-EF2	GTAAGGAAATGAGACGAC	STS-Seq
AtccmB-ER2	GTAACATGGAAAACCAC	STS-Seq
ATMNAD5-F1	ATGTATCTACTTATCGTATTGGCCC	STS-Seq
ATMNAD5-R1	TTATTCTGACTTGACTTGTATAAAAAC	STS-Seq
ATMNAD1-F1	ATGTACATAGCTGTTCCAGCTGAAAT	STS-Seq
ATMNAD4-F1	ATGTTAGAACATTCTGTGAATGC	STS-Seq
ATMNAD4-R1	TCAATGAAATTGCCATGTTGCAC	STS-Seq
Atnad7-F2	TTGGTACTGTCACTGCACAG	STS-Seq
ATMNAD7-R1	CTATCTATCCACCTCTCCAAACAC	STS-Seq
qAtrpl2-e1-2-F	CCGAAGACGGATCAAGGTAA	qRT-PCR
qAtrpl2-i1-F	TGCTTCTCTAATAGCCCCGT	qRT-PCR
qAtrpl2-e1-2-R	CGCAATTCATCACCAATTG	qRT-PCR
qAtrps3-e1-2-F	CCGATTCGGTAAGACTTGG	qRT-PCR
qAtrps3-i1-F	TCTACGGCGGGGTCACTAT	qRT-PCR
qAtrps3-e1-2-R	AGCCGAAGGTGAGTCTCGTA	qRT-PCR
qAtcox2-e1-2-F	TGATGCTGTACCTGGTCGTT	qRT-PCR
qAtcox2-i1-F	AGCAGTACGAGCTGAAAGGC	qRT-PCR
qAtcox2-e1-2-R	TGGGGGATTAATTGATTGGA	qRT-PCR
qAtccb452-e1-2-F	CACATGGAGGAGTGTGCATC	qRT-PCR
qAtccb452-i1-R	CCCGGATCGAACATCAGAGTT	qRT-PCR
qAtccb452-e1-2-R	GTGGGTCCATGTAAATGATCG	qRT-PCR
qAtnad1-e1-2-F	TTGCCATATCTCGCTAGGTG	qRT-PCR
qAtnad1-i1-F	CGTGCTCGTACGGTTCATAG	qRT-PCR
qAtnad1-e1-2-R	GACCAATAGATACTTCATAAGAGACCA	qRT-PCR
qAtnad1-e2-3-F	TCTGCAGCTCAAATGGTCTC	qRT-PCR
qAtnad1-i2-R	GGTTGGGTTAGGGAACATC	qRT-PCR
qAtnad1-e2-3-R	ATTCAGCTTCCGCTTCTGG	qRT-PCR
qAtnad1-e3-4-F	TCCGTTGATCTCCCAGAAG	qRT-PCR
qAtnad1-i3-F	GGGAGCTGTATGAGCGGTAA	qRT-PCR
qAtnad1-e3-4-R	AAAAGAGCAGACCCCATTGA	qRT-PCR
qAtnad1-e4-5-F	TCTTCAATGGGGTCTGCTC	qRT-PCR
qAtnad1-i4-F	ACGGAGCTGCATCCCTACT	qRT-PCR
qAtnad1-e4-5-R	AGCCCGGGATCTTCTTGA	qRT-PCR

qAtnad2-e1-2-F	GGATCCTCCCACACATGTC	qRT-PCR
qAtnad2-i1-F	CCCATTCTAACCAAGTGGAG	qRT-PCR
qAtnad2-e1-2-R	GCGAGCAGAACAGAAGGTTAT	qRT-PCR
qAtnad2-e2-3-F	AATATTGATCTTAGGTGCATTTC	qRT-PCR
qAtnad2-i2-R	CCCGATCCGATAGTTACAA	qRT-PCR
qAtnad2-e2-3-R	AAAGGAACTGCAGTGATCTGA	qRT-PCR
qAtnad2-e3-4-F	CTATGGGTCTACTGGAGCTACCC	qRT-PCR
qAtnad2-i3-F	GGCGAATTCAAACCTGTGG	qRT-PCR
qAtnad2-e3-4-R	GCGCAATAGAAAGGAATGCT	qRT-PCR
qAtnad2-e4-5-F	TATTGTTCTCGCCGCTT	qRT-PCR
qAtnad2-i4-R	CTTATTCTGGCACACCTCC	qRT-PCR
qAtnad2-e4-5-R	CAAAGGAGAGGGTATAGCAA	qRT-PCR
qAtnad4-e1-2-F	ATTCTATGTTTCCCAGAAAGC	qRT-PCR
qAtnad4-i1-F	CCGTATGATGCGGAAGTCTC	qRT-PCR
qAtnad4-e1-2-R	GAAAAACTGATATGCTGCCTTG	qRT-PCR
qAtnad4-e2-3-F	AATAACCATGTTCCCGAAG	qRT-PCR
qAtnad4-i2-F	GCGGAACGACCAGAAAAATA	qRT-PCR
qAtnad4-e2-3-R	TGCTACCTCCAATTCCCTGT	qRT-PCR
qAtnad4-e3-4-F	TTCCTCCATAAAATTCTCCGATT	qRT-PCR
qAtnad4-i3-F	TCTAGCTGGTTCGGAGAGC	qRT-PCR
qAtnad4-e3-4-R	TGAAATTGCCATGTTGCAC	qRT-PCR
qAtnad5-e1-2-F	CCATGGATCTCATCGGAAAT	qRT-PCR
qAtnad5-i1-F	TTCGCAAATAGGTCCGACT	qRT-PCR
qAtnad5-e1-2-R	TGGACCAAGCTACTTATGGATG	qRT-PCR
qAtnad5-e2-3-F	CTGGCTCTCGGGAGTCTCTT	qRT-PCR
qAtnad5-i2-F	GTACGATCGTGTGGGTGA	qRT-PCR
qAtnad5-e2-3-R	TACCTAAACCAATCATCATATC	qRT-PCR
qAtnad5-e3-4-F	GATATGATGATTGGTTAGGTA	qRT-PCR
qAtnad5-i3-F	GCCGTGTAATAGGCGACCA	qRT-PCR
qAtnad5-e3-4-R	AACTCGGATTCGGCAAGAA	qRT-PCR
qAtnad5-e4-5-F	GTTCCTCGCGTTCGGATAT	qRT-PCR
qAtnad5-i4-F	CCTGTAAACCCCCATGATGT	qRT-PCR
qAtnad5-e4-5-R	AACATTGCAAAGGCATAATGA	qRT-PCR
qAtnad7-e1-2-F	ACCTCAACATCCTGCTGCTC	qRT-PCR
qAtnad7-i1-F	ACGGTTTTAGGGGATCTG	qRT-PCR
qAtnad7-e1-2-R	AAGGTAAAGCTGAAGATAAGTTGT	qRT-PCR
qAtnad7-e2-3-F	GAGGGACTGAGAAATTAATAGAGTACA	qRT-PCR
qAtnad7-i2-F	AGTGGGAGAGCCGTGTTATG	qRT-PCR
qAtnad7-e2-3-R	TGGTACCTCGCAATTCAAAA	qRT-PCR
qAtnad7-e3-4-F	ACTGTCACTGCACAGCAAGC	qRT-PCR
qAtnad7-i3-F	TAAAGTGAAGTGGTGGCCT	qRT-PCR
qAtnad7-e3-4-R	CATTGCACAAATGATCCGAAG	qRT-PCR
qAtnad7-e4-5-F	GATCAAAGCCGATGATCGTAA	qRT-PCR
qAtnad7-i4-F	CGGCCAAATGACTACAGGAT	qRT-PCR
qAtnad7-e4-5-R	AGGTGCTTCAACTGCGGTAT	qRT-PCR
G3-LP	GTCGGAAGTAAGGTACCTCC	Genotyping

LBb1.3	ATTTGCCGATTCGGAAC	Genotyping
G3-R4	AAGGGCAACGAACGTAGTAG	Genotyping
B2-F1	ATTTGGAGAGAACACGGGG	Genotyping
G3-R1	ATCTCCGATCCTCCAGCTT	Genotyping
B3-SF1	TGTGGAATTGTGAGCGGATA	Genotyping
P2S1-R1	GCAGACGAGGAACAACTTGT	Genotyping

Materials and Methods

Complementation of Mutants

To complement the mutants under the control of seed specific promoter, the 2000 bp promoter region of *At2S1* was fused with the coding regions of *GRP23* and *MEF8S* at their 5' termini by PCR and the resulting fragments were cloned into pGWB1 vectors. To complement *grp23* mutant with *GRP23*-3MYC fusion, the coding region of *GRP23* was cloned into pGWB17 vector. To complement *grp23* with *GRP23*-TurboID fusion, the coding region of *GRP23* was fused with ORF of TurboID at 3' terminus by PCR and the resulting fragments were cloned into pGWB1 vector. The constructs were transferred into *Agrobacterium tumefaciens* EHA105 and transformed into the corresponding heterozygous T-DNA insertion plants by floral dip (1). Transformed plants were selected on MS plats containing hygromycin B resistance. T2 or T3 homozygous plants were used for experiments.

Y2H

The sequences of interest genes encoding the mature proteins were cloned into the pGADT7 (AD) and pGBK7 (BD) vectors. Y2HGold yeast strain was co-transformed with AD-interest and BD-interest constructs. Empty vectors were used as negative controls. Transformed yeast cells were selected on agar medium plates lacking leucine and tryptophan (SD-TL). Single transformants were grown in liquid SD-TL media overnight before they were diluted with liquid SD-TL media to OD₆₀₀= 0.5. 7 µl of dilutions were dropped onto the agar medium plates lacking leucine, tryptophan, histidine, and adenine (SD-TLHA) and SD-TLHA supplemented with X-α-Gal. The results were recorded after 3 days of incubation at 30 °C.

BiFC and Subcellular Localization

The complete coding sequences of interest were cloned into BiFC vectors pSPYNE and pSPYCE (2), respectively, to enable the expression of proteins of interest fused either to the N-terminal 155 amino acids of YFP (nYFP) or to the C-terminal 86 amino acids of YFP (cYFP). Constructs were co-transfected into *Arabidopsis* protoplasts as previously described (3). The protoplasts were incubated under weak light for 18-22 hours, and the YFP fluorescence was determined using a Zeiss LSM 880 confocal microscope under the same setting. Mitochondria were stained with MitoTracker Red. Each combination was repeated three independent times with similar results.

The full coding sequence of *GRP23* was cloned into pGWB5 vector to express *GRP23*-GFP fusion under the control of CaMV 35S promoter. The resulting construct was transferred into EHA105. *Agrobacterium* cells containing pGWB5-*GRP23* was adjusted with infiltration buffer (10 mmol/L MgCl₂, 10 mmol/L MES (pH 5.6), 200 mmol/L Acetosyringone) to OD₆₀₀= 0.5 before infiltration. Young leaves of 4-week-old *N. benthamiana* were infiltrated with the cultures. At 22-24 hours after infiltration, small pieces of infiltrated leaves were excised, soaked with PBS containing 100 nM Mito Tracker Red and 10 µg/ml DAPI for 1 hour, and observed under a Zeiss LSM 880 confocal microscope.

Organelle purification and Western Blot

To obtain mitochondrial proteins, 10g roots of 35S::*GRP23*-3MYC complemented *grp23* plants or

Col-0 were ground at 4°C in extraction buffer (0.3 M Suc, 5mM tetrasodium pyrophosphate, 10mM KH₂PO₄, pH 7.5, 2 mM EDTA, 1% [w/v] polyvinylpyrrolidone 40, 1% [w/v] BSA, 5 mM Cys, and 20 mM ascorbic acid). The homogenate was centrifuged for 5 min at 3,000 g to remove cell debris, and the supernatant was centrifuged for 10 min at 20,000 g. The pellet was resuspended in ice-cold wash buffer (0.3 M Suc, 1 mM EGTA, and 10 mM MOPS/KOH, pH 7.2) twice and crude mitochondria were solubilized in 2×SDS sample buffer.

To obtain chloroplast proteins, 10g leaves of 35S::GRP23-3MYC complemented *grp23* plants or Col-0 were ground at 4°C in extraction buffer (50 mM HEPES-NaOH, pH 8, 2 mM EDTA, 0.3 M mannitol, 1% (w/v) bovine serum albumin, and 2 mM DTT). Chloroplasts were isolated using a 50% Percoll gradient at 6,500 g for 15 min. Intact chloroplasts were collected, washed twice in wash buffer (50 mM HEPES-NaOH, pH 8, 2 mM EDTA, and 0.3 M mannitol), and solubilized in 2×SDS sample buffer.

To obtain nuclear proteins, 10g leaves of 35S::GRP23-3MYC complemented *grp23* plants or Col-0 were ground at 4°C in ice-cold homogenization buffer (0.01M trizma base, 0.08M KCl, 0.01M EDTA, 1Mm spermidine, 1 mM spermine, final pH 9.5). The homogenate was centrifuged for 5 min at 500 g, and Triton X-100 at a final concentration of 0.5% was added to the supernatant. The homogenate was pelleted by centrifugation at 1800 g for 20 min, and then the pellet was washed by ice-cold wash buffer twice. Nuclei were solubilized in 2×SDS sample buffer.

Proteins were separated by SDS-PAGE, transferred to nitrocellulose membranes, and subjected to immunoblotting using antibodies against the MYC tag (Sigma), the nuclear histone H3, the chloroplast D1 (4), and the mitochondrial Nad9 (5).

TurboID-mediated Proximity Labeling

The *grp23* mutants complemented by 35S::GRP23-TurboID were treated by 50 μM biotin for 4 hour. 2 g roots of treated plants were ground to fine powder with liquid nitrogen, and then the powder was suspended with 2 ml lysis buffer (50 mM Tris, pH 7.5, 300 mM sucrose, 1% Triton X-100, cComplete EDTA-free protease inhibitors (Roche), and centrifuged at 12,000 g for 15 min. The supernatant was subjected to Zeba Spin Desalting Columns to remove free biotin. The resulting proteins were incubated with 100 μL Dynabead M-280 Streptavidin beads (Thermo Fisher Scientific, Waltham, MA) at 4 °C for 2 hours, and then the beads were washed 3 times with wash buffer (50 mM Tris, pH 7.5, 0.1% Triton X-100, cComplete EDTA-free protease inhibitors (Roche)). The biotinylated proteins were eluted by 2×SDS sample buffer and separated by SDS-PAGE. The entire gel lane was cut and digested with trypsin, and the extracted peptides were analyzed by a Q-Exactive mass spectrometry (Thermo Fisher Scientific) coupled to an EASY-nLC 1000 (Thermo Fisher Scientific).

RNA editing analysis

Total RNA was extracted from leaves or entire seedlings using the Qiagen Plant RNeasy kit (Qiagen) according to the manufacturer's instructions and followed by a treatment with DNase I (New England BioLabs) to remove genomic DNA contamination. Reverse transcription reactions were performed with random hexamers by SuperScript II Reverse Transcriptase (Invitrogen). Primers to amplify the mitochondrial and plastid transcripts are described in Table S2. The RT-PCR amplicons were mixed in equimolar proportions and then sheared by sonication to generate 350 bp fragments. Sequencing libraries were generated using Truseq Nano DNA HT Sample preparation

Kit (Illumina USA) following manufacturer's recommendations. Sequencing was performed by Illumina NovaSeq platform and 150 bp paired-end reads were generated with insert size around 350 bp. Sequencing data was analyzed by VarScan2 program. The difference threshold for editing extent is defined as: $(T/(C+T)\% \text{ in mutant} - T/(C+T)\% \text{ in WT}) \geq 20\%$.

The amplicons were directly sequenced to verify their editing extents as well. The editing efficiency between the mutant and Col-0 was compared by SEQUENCHER 4.14 software (SoftGenetics, Cambridge, MA, USA).

References

1. S.J. Clough, A.F. Bent, Floral dip: A simplified method for Agrobacterium mediated transformation of *Arabidopsis thaliana*. *Plant J.* **16**, 735-743 (1998).
2. C.D. Hu, Y. Chinenov, T.K. Kerppola, Visualization of interactions among bZIP and Rel family proteins in living cells using bimolecular fluorescence complementation. *Mol. Cell* **9**, 789-798 (2002).
3. S.D. Yoo, Y.H. Cho, J. Sheen, Arabidopsis mesophyll protoplasts: a versatile cell system for transient gene expression analysis. *Nat. Protoc.* **2**, 1565-72 (2007).
4. X.Y. Liu *et al.*, ZmPPR26, a DYW-type pentatricopeptide repeat protein, is required for C-to-U RNA editing at *atpA-1148* in maize chloroplasts. *J. Exp. Bot.* **72**, 4809-4821 (2021).
5. Y.Z. Yang *et al.*, EMP32 is required for the *cis*-splicing of *nad7* intron 2 and seed development in maize. *RNA Biol.* **18**, 499-509 (2021).